



Mohamed Khider University of Biskra
Faculty of Science and Technology
Department of Electrical Engineering

Master's Thesis

Science and Technology
Electromecanic

Ref. :

Presented and defended by:
BEN LALMI Taha
GHERIB Hassen Nacer Allah

On June, 2025

Conceptual Design of a High-Temperature, High-Pressure wireless downhole pressure and Temperature gauge for harsh environments

Jury :

M.	MIMOUNE SOURI Mohamed	Pr	University of Biskra	President
Mme.	HADRI HAMIDA Amel	Pr	University of Biskra	Supervisor
Mme.	BENYAHIA Naima	MCB	University of Biskra	Examiner

Academic Year : 2024 - 2025



Mohamed Khider University of Biskra
Faculty of Science and Technology
Department of Electrical Engineering

Master's Thesis

Science and Technology
Electromecanic

Ref. : Entrez la référence du document

Conceptual Design of a High-Temperature, High-Pressure wireless downhole pressure and Temperature gauge for harsh environments

On : June, 2025

Presented by :

**BEN LALMI Taha
GHERIB Hassen Nacer Allah**

Favorable opinion of the supervisor:

Signature Favorable opinion of the Jury President

Stamp and signature

Acknowledge

First and foremost, I thank God Almighty for granting me the strength, patience, and guidance throughout the completion of this work.

I would like to express my sincere gratitude to my supervisor, Prof. HADRI HAMIDA Amel, for her continuous support, valuable guidance, and scientific insight throughout all stages of this thesis.

I would also like to thank Prof. MIMOUNE SOURI Mohamed, President of the jury, for accepting to lead the defense session and for his time and consideration in evaluating this work.

My gratitude also goes to Dr. BENYAHIA Naima, Examiner, for her interest in this research and for her academic input and remarks that will certainly contribute to its improvement.

Finally, I thank all the professors of the department of Electrical Engineering for the knowledge and support they provided throughout my academic journey.

Dedication

This work is dedicated to my parents, whose unwavering guidance and belief in my aspirations have been the bedrock of this academic journey.

To my brothers Adel, Mansour, Akram, and Chaouki, and my sisters Tahani, Hanifa, Sara and to their families thank you for the consistent support and the grounding presence of our shared bond. I also extend my gratitude to my uncle, Hada, for his wisdom and encouragement throughout.

A silent acknowledgment is given to the profound connection that quietly inspires my endeavors, a truth felt deeply within my favorite person.

To my binome, Nasrallah, your collaborative spirit and insightful partnership have been invaluable to this research. And to my dear friends, whose steadfast encouragement provided strength and perspective through every challenge.

BEN LALMI Taha.

Dedication

*To the ones who have always been my support and strength,
To those who raised me with values and surrounded me with love
and prayers,*

*To my dear parents, I dedicate this work as a token of gratitude
and love.*

*To my siblings, my lifelong companions and supporters in difficult
times,*

*Thank you for your constant presence that gave me strength and
perseverance.*

*And to my loyal friends, who stood by me throughout this academic
journey,*

*I share with you the fruit of this effort, hoping to always live up to your
trust*

GHERIB Hassen Nacer Allah.

Summary:

HPHT wells demand temperatures ≥ 150 °C and pressures $\geq 10\,000$ psi, with real-time downhole measurements essential for safety, production optimization, and failure prevention. Quartz, sapphire, and memory gauges operate under these harsh conditions, facing narrow mud-weight windows, borehole elasticity, and gas liberation. Data is transmitted via wireline logging and intelligent drill pipe, and wirelessly by low-frequency EM waves, acoustic telemetry through the drill string, or mud pulses, while fiber optics deliver continuous high-rate monitoring. Systems are compared on data rate, max depth, signal integrity, and cost. MATLAB 2015a simulations reveal that adding repeaters and advanced encoding/decoding achieves ≥ 99 % data recovery

Keywords: HPHT wells, downhole gauges, real-time monitoring, electromagnetic telemetry, acoustic telemetry, mud-pulse transmission, fiber-optic sensing, data rate, signal integrity, MATLAB simulation

الملخص:

آبار الضغط والحرارة العاليتين تتطلب درجات حرارة ≤ 150 °C وضغط $\leq 10\,000$ psi ، ومن الضروري إجراء قياسات آنية من عمق البئر لضمان السلامة وتحسين الإنتاج وتجنب الحوادث. تُستخدم مجسات كوارتز وسافير وأجهزة ذاكرة لقياس الضغط والحرارة في البيئات القاسية، ويواجه التشغيل تحديات مثل ضيق نافذة وزن الطين، وتمدد وانكماش جدران البئر، وتحرر الغازات. تُنقل البيانات سلكياً عبر وايرلاين وأنايبب ذكية مزودة بكوابل، ولاسلكياً بموجات كهرومغناطيسية منخفضة التردد أو موجات صوتية في عمود الحفر أو نبضات الطين، ويمكن استخدام الألياف البصرية لمراقبة مستمرة بمعدلات عالية. تُقارن الأنظمة وفق معدل البيانات والعمق الأقصى وجودة الإشارة والتكلفة. محاكيات MATLAB 2015a تُظهر أن إضافة مكررات وتقنيات تشفير وفك متطورة يرفعون دقة استرجاع البيانات إلى ≤ 99 %.

الكلمات المفتاحية: آبار الضغط والحرارة العاليتين، مجسات كوارتز وسافير، القياس الفوري، الاتصالات الكهرومغناطيسية، القياس الصوتي، نبضات الطين، الألياف البصرية، معدل البيانات، جودة الإشارة، محاكيات

MATLAB

Résumé:

Les puits HPHT exigent des températures ≥ 150 °C et des pressions $\geq 10\,000$ psi, avec des mesures en temps réel indispensables pour la sécurité, l'optimisation de la production et la prévention des incidents. On utilise des capteurs quartz, saphir et gauges à mémoire dans ces conditions extrêmes, et l'exploitation doit gérer une fenêtre de densité de boue étroite, la dilatation/contraction du puits et le dégazage. Les données se transmettent filairement via wireline et tubage intelligent, et sans fil par ondes électromagnétiques basse fréquence, ondes acoustiques dans la colonne ou impulsions de boue, tandis que la fibre optique permet une surveillance continue à haut débit. Les solutions se comparent selon le débit, la profondeur maximale, l'intégrité du signal et le coût. Les simulations MATLAB 2015a montrent que l'ajout de répéteurs et le codage/décodage optimisés assurent une récupération de données ≥ 99 %.

Mots-clés: puits HPHT, capteurs quartz/saphir/mémoire, mesure en temps réel, télémétrie électromagnétique, télémétrie acoustique, transmission par boue, fibre optique, débit de données, intégrité du signal, simulation MATLAB

Table of Contents:

Acknowledge

Dedication

Summary

الملخص

Résumé

Table of Contents

List of figures

List of tables

List of Abbreviations

General introduction 1

Chapter I: The HPHT wells and gauges

I.1) Introduction: 3

I.2) Definition of HPHT Wells: 3

 I.2.1) ENI Definition 3

 I.2.2) HSAP (Halliburton–Saudi Aramco Production) Definition 4

I.3) Clasification of HPHTwells 4

I.4) Working conditions for HPHT 5

I.5) Challenges Of HPHT wells 6

 I.5.1) Slow Progress in Productive Formation: 6

 I.5.2) Well Control 6

 I.5.3) Pressure Challenges 7

 I.5.4) Temperature Challenges: 9

I.6) Oil & Gas Well Types 11

 I.6.4) Other types of wells 11

I.7) Drilling Techniques 12

I.8) Steps And Phases For Drilling Oil And Gas Wells: 12

I.8.1) Planning & Preparation:	12
I.8.2) Mobilization:.....	13
I.8.3) Spud & Conductor Installation:.....	13
I.8.4) Surface-Hole Drilling:	13
I.8.5) Intermediate-Hole Drilling:	13
I.8.6) Production-Hole Drilling:	13
I.8.7) Completion Operations:.....	14
I.8.8) Testing & Evaluation:.....	14
I.8.9) Production Start-Up:	14
I.8.10) Monitoring & Maintenance:	14
I.8.11) Plugging & Abandonment (P&A):	14
I.9) Downhole Gauges:	15
I.9.1) The Importance of Downhole Gauges	16
I.9.2) Pressure and temperature gages	16
I.10) Type of gauges:	16
I.10.1) Quartz Crystal Gauges:	16
I.10.2) Sapphire/Piezoresistive Gauges:	17
I.10.3) Permanent Downhole Monitoring Systems:.....	17
I.10.4) Memory Gauges:.....	17
I.10.5) Signature quartz gauge:	17
I.11) Conclusion:.....	21

Chapter II: Data transmission

II.1) Introduction:.....	23
II.2) Wire communication downhole data:	23
II.2.1) Traditionally Wireline logging:	23
II.2.2) Wired Pipe line:	24
II.2.3) Optic fibry transmission :	26

II.3) Wireless communication downhole data:	26
II.3.1) Electromagnetic Telemetry:	26
II.2.2) Acoustic wave	29
a) Principe of Acoustic wave	29
b) Components and Operation	29
c) Schemes for Modulation Typical schemes include	31
II.2.3) Mud pulse telemetry (MPT) system:	32
a) Principle of Operation:	32
b) Modulation and Data Encoding:	32
II.2.4) Other Possible Downhole Telemetry Types:	33
II.4) Comparison of telemetry systems:	34
II.5) Future Development Trends:	35
II.5.1) Leveraging AI and Big Data for Valve Management:	35
II.5.2) Harnessing 5G and IoT Connectivity:	35
II.5.3) Diagnostics of Faults and Predictive Maintenance:	36
II.6) Conclusion:	36

Chapter III: Simulation of HPHT Downhole Wireless Telemetry

III.1) Introduction:	38
III.2) Simulation of HPHT well telemetry in Real-time:	39
III.2.1) Electromagnetic wave using MATLAB:	39
III.2.2) Acoustic wave using MATLAB:	50
With repeters	51
Without repeters (we delete the repeter gain)	56
III.2.3) Pressure wave (pulse wave) using MATLAB:	60
III.3) Compariton of simulation settings and results:	68
III.3.1) Calculation Details:	69
a) EM Waves:	69

b) Acoustic (With Repeaters):	69
c) Acoustic (Without Repeaters):.....	69
d) Pressure Pulse:	70
III.4) Conclusion:	70
General conclusion:	71
References:	72

List of figures:

Figure I.1: Definition of HPHT points - Graph: $T = f(GP)$	4
Figure I.2: The different types of HPHT	5
Figure I.3: Pressure gradients. The hydrostatic pressure gradient (black line), assuming seawater, is 0.43 psi/ft [9.79 kPa/m]; it follows a straight line.	9
Figure I.4: Earth's geothermal gradient.	10
Figure I.5: vertical and horizontal drilling.	12
Figure I.6: Typical Hydrocarbon Production Well with Multiple Casing Strings including two Intermediate Casing Strings	15
Figure I.7: Signature gauge.	19
Figure I.8 : Quartz Memory Tool gauge	28
Figure II.1: Cutaway view of the telemetry drill pipe system in a drill pipe connection.	24
Figure II.2: The non-contact line coupler uses induction to transmit data from one connection to another.	25
Figure II.3: Data transmission concept by using intelligent drill pipe telemetry.	25
Figure II.4: Electromagnetic Waves.	27
Figure II.5: Example of electromagnetic telemetry in a well	28
Figure II.6: Longitudinal waves in a spring are a good analogy for compressional acoustic waves in the tubing string of a well.	30
Figure II.7: Flow-chart of acoustic telemetry system operation	31
Figure II.8: Signal flow of mud pulse telemetry	33
Figure III.1: Simulation of EM telemetry system using MATLAB	39

Figure III.2: Simulation of Encryption temperature subsystem for 8 bits	41
Figure III.3: result of Encryption temperature subsystem for 8 bits	42
Figure III.4: Simulation of Encryption pressure subsystem for 16 bits	42
Figure III.5: result encryption pressure subsystem for 16 bits	43
Figure III.6: the temperature in downhole sensor for EM waves (step input)	46
Figure III.7: the temperature in space for EM waves (step output)	47
Figure III.8: pressure in the downhole for EM waves (step input)	47
Figure III.9: pressure in the workspace for EM waves (step output)	48
Figure III.10: the temperature in downhole sensor for EM waves (sine wave input)	48
Figure III.11: the temperature in workspace for EM waves (sine wave output)	49
Figure III.12: the Pressure in downhole sensor for EM waves (sine wave input)	49
Figure III.13: the temperature in workspace for EM waves (sine wave output)	50
Figure III.14: Simulation of second zone of acoustic wave telemetry	51
Figure III.15: the temperature in downhole sensor with repeters for acoustic waves (step input)	51
Figure III.16: the temperature in workspace with repeters for acoustic waves (step output)	52
Figure III.17: the Pressure in downhole sensor with repeters for acoustic waves (step input)	52
Figure III.18: the pressure in workspace with repeters for acoustic waves (step output)	53
Figure III.19: the temperature in downhole sensor with repeters for acoustic waves (sin wave input)	53

Figure III.20: the temperature in workspace with repeters for acoustic waves (sin wave output)	54
Figure III.21: the Pressure in downhole sensor with repeters for acoustic waves (sin wave input)	54
Figure III.22: the pressure in workspace with repeters for acoustic waves (sin wave output)	55
Figure III.23: Simulation of second zone of acoustic wave telemetry without repeter	56
Figure III.24: the temperature in downhole sensor without repeters for acoustic waves (step input)	56
Figure III.25: the temperature in workspace without repeters for acoustic waves (step output)	57
Figure III.26: the Pressure in downhole sensor without repeters for acoustic waves (step input)	57
Figure III.27: the pressure in workspace without repeters for acoustic waves (step output)	58
Figure III.28: the temperature in downhole sensor without repeters for acoustic waves (sin wave input)	58
Figure III.29: the temperature in workspace without repeters for acoustic waves (sin wave output)	59
Figure III.30: the Pressure in downhole sensor without repeters for acoustic waves (sin wave input)	59
Figure III.31: the pressure in workspace without repeters for acoustic waves (sin wave output)	60
Figure III.32: Simulation of pressure wave telemetry system using MATLAB	61
Figure III.33: Similation of Encryption flow for subsystem for 4 bits	62
Figure III.34: the temperature in downhole sensor for pressure waves (step input)	62
Figure III.35: the temperature in space for pressure waves (step output)	63
Figure III.36: the Pressure in downhole sensor for pressure waves (step input)	63

Figure III.37: the pressure in workspace for pressure waves (step output)	64
Figure III.38: the flow in downhole sensor for pressure waves (step input)	64
Figure III.39: the flow in workspace for pressure waves (step output)	65
Figure III.40: the temperature in downhole sensor for pressure waves (sin wave input)	65
Figure III.41: the temperature in space for pressure waves (sin wave output)	65
Figure III.42: the Pressure in downhole sensor for pressure waves (sin wave input)	66
Figure III.43: the Pressure in downhole sensor for pressure waves (sin wave output)	65
Figure III.44: the flow in downhole sensor for pressure waves (sin wave input)	67
Figure III.45: the flow in workspace for pressure waves (sin wave output)	67

List of tables:

Table II.1: A comparative between different data transmission technologies.	34
Table III.1: Comparison Table of Error Constants, Accuracy Rate, Response Speed, and Stability for HPHT Well Telemetry Systems	68

List of Abbreviations:

AI: Artificial Intelligence

BHA: Bottom Hole Assembly

BHT: Bottom Hole Temperature

DST: Drill Stem Test

EOR: Enhanced Oil Recovery

EMT: Electromagnetic Telemetry

ELF: Extremely Low Frequency

ENI: Ente Nazionale Idrocarburi (Italian multinational oil and gas company)

FOWM: Fibre Optic Well Monitoring

FDMA: Frequency Division Multiple Access

FSK: Frequency-Shift Keying

GP: Gradient Pressure

HPHT: High Pressure High Temperature

HSAP: Halliburton–Saudi Aramco Production

HSE: Health, Safety, and Environment

IoT: Internet of Things

LWD: Logging While Drilling

MPT: Mud Pulse Telemetry

MCM: Multichip Module

NPD: Norwegian Petroleum Directorate

OBM: Oil-Based Mud

P&A: Plugging and Abandonment

PDG: Permanent Downhole Gauge

PSK: Phase-Shift Keying

SOI: Silicon-on-Insulator

TD: Total Depth

TVD: True Vertical Depth

WHP: Wellhead Pressure

General Introduction

The exploration and extraction of hydrocarbons from High-Pressure High-Temperature (HPHT) wells have become pivotal to meeting global energy demands, yet they present formidable technical challenges. Demand precise real-time monitoring of downhole conditions to ensure operational safety, optimize production, and prevent catastrophic failures. Traditional measurement methods in conventional wells require halting production and waiting days for stabilization—a process that is inefficient, costly, and impractical in HPHT environments. The inability to obtain instantaneous data compromises reservoir management, delays critical decision-making, and heightens risks of blowouts or equipment failure.

This thesis addresses these challenges by investigating advanced telemetry systems capable of transmitting real-time pressure and temperature data from extreme downhole environments to the surface. Focusing on electromagnetic, acoustic, and mud pulse technologies, the study evaluates their performance under HPHT conditions through MATLAB simulations. Key objectives include analyzing signal attenuation, transmission delays, and accuracy to identify optimal solutions for continuous monitoring. By bridging the gap between theoretical frameworks and practical applications, this work aims to enhance the reliability of downhole data acquisition, enabling safer and more efficient hydrocarbon extraction. The findings contribute to the broader goal of advancing intelligent oilfield technologies, ensuring sustainable operations in increasingly complex reservoirs.

In Chapter I, we review the characteristics of these wells and the measurement devices used. Then, in Chapter II, we examine data transmission systems from the depths to the surface, providing a detailed analysis of wired and wireless techniques. Third, in Chapter III, we simulate the performance of these systems using MATLAB to test their reliability in harsh environments. Finally, we conclude this work with a conclusion.

Chapter I:

The HPHT wells and gauges

I.1) Introduction:

One of the most highly sophisticated areas of the energy business is the exploration and production of petroleum. The intricate constructions known as oil and gas wells, which are bored deep into the ground to reach hydrocarbon resources, are at the center of these activities. It is crucial for geologists, engineers, and energy experts to comprehend how wells work, how petroleum is extracted, and how vital data is obtained from these subterranean networks.

Using gauges is one of the most important aspects of well monitoring and management. These high-precision tools are used in wells to measure vital variables including fluid composition, temperature, and pressure. Ensuring well integrity, maximizing output, and averting catastrophic failures all depend heavily on the precise interpretation of these factors. This chapter provides a thorough grasp of the principles of petroleum production by introducing the idea of gauges, explaining how they operate, and examining the many kinds of wells.

I.2) Definition of HPHT Wells:

High Pressure High Temperature (HPHT) wells are classified according to certain temperature and pressure thresholds that change dependent on the classification standards established by various service providers and industry participants. The essential definitions offered by significant organizations in the petroleum industry are listed below:

I.2.1) ENI Definition:

ENI states that a well is considered HPHT if it satisfies one or both of the following requirements:

- The gradient pressure (GP) is greater than 1.81 kg/cm² every 10 meters (equal to 0.8 psi/ft) or the wellhead pressure (WHP) surpasses 10,000 psi, or roughly 690 bar.
- The BHT (bottom hole temperature) exceeds 300°F (150°C).

According to the definition provided by the Norwegian Petroleum Directorate (NPD), a well is classified as HPHT if its true vertical depth (TVD) is greater than 5,000 meters [1] .

Chapter I : The HPHT wells and gauges

I.2.2) HSAP (Halliburton–Saudi Aramco Production) Definition:

An HPHT well is classified as such if its reservoir temperature is 350°F or higher, or if its fracture pressure is more than 15,000 psi.

These varying definitions highlight the lack of a globally accepted threshold for HPHT wells, which is indicative of the complexity of well design and the risk assessment standards used by different operators. Because it directly affects the choice of materials, well design, and safety procedures during drilling and production operations, the categorization is essential [1] .

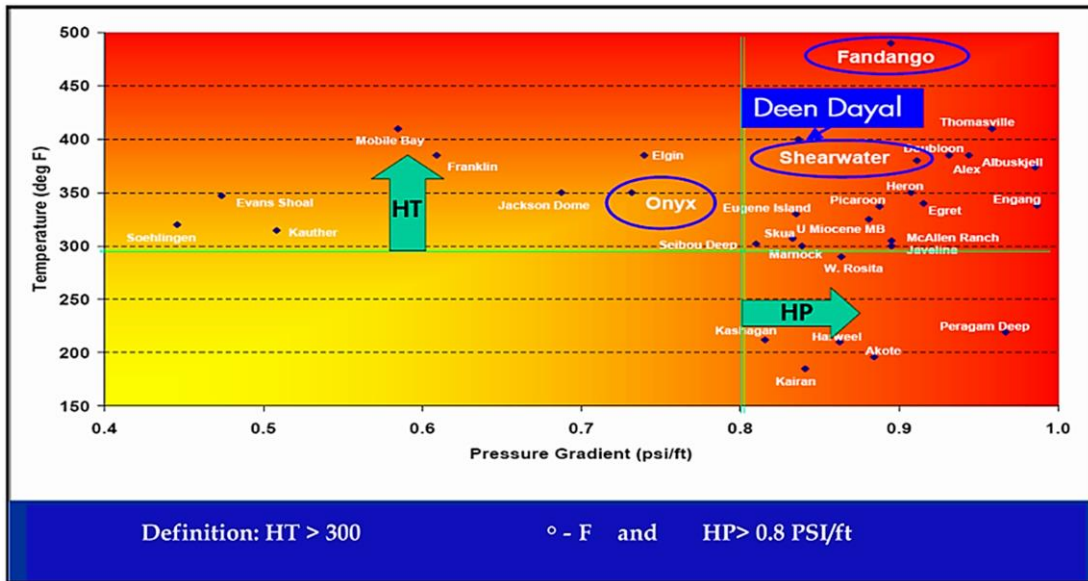


Figure I.1: Definition of HPHT points - Graph: $T = f(GP)$ [1]

I.3) Classification of HPHT wells:

Classifications have been created in order to identify HPHT working settings, carry out operations securely, and fill up technological gaps. These divisions divide HPHT activities into three primary tiers.

Wells classified as Level I have reservoir temperatures between 149°C and 204°C (300°F and 400°F) and/or initial reservoir pressures between 10,000 psi and 20,000 psi. The majority of HPHT activities are currently categorized as Level I, including several deep-water HPHT gas/oil wells and shale resources

Chapter I : The HPHT wells and gauges

A well-known HPHT field in Norway is the Kristin field, which has a reservoir pressure of 13,200 psi and a temperature of about 177°C (350°F).

Level II HPHT, often known as "Ultra" HPHT, covers any reservoir with temperatures between 204°C and 260°C (400°F and 500°F) and/or pressures between 20,000 and 30,000 psi.

This includes a number of deep gas fields on the continental shelf of the Gulf of Mexico and on American soil.

Level III includes "extreme" HPHT wells, which have reservoir temperatures between 260°C and 315°C (500°F and 600°F) and/or pressures between 30,000 psi and 40,000 psi.

The HPHT sector with the biggest technological limitations is Level III. [2]

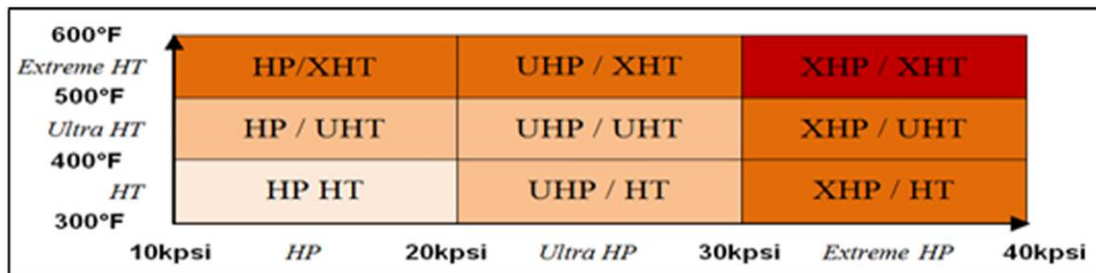


Figure I.2 : The different types of HPHT [2]

I.4) Working conditions for HPHT:

It comes with the necessary tools, specialized equipment, and training to operate in HPHT environments. Effective operations need careful planning, and in order to handle HPHT problems, updated operational procedures are frequently required. While mistakes made in conventional wells can sometimes lead to lost time, extraordinary care is needed to avoid catastrophic consequences for HPHT operations' personnel and equipment.

The petroleum industry is still able to operate in deeper depths and hotter wells thanks to the continuous finding of new hydrocarbon sources, the development of instruments to fit HPHT conditions, and understanding on how to deal with such circumstances [3].

I.5) Challenges Of HPHT wells:

I.5.1) Slow Progress in Productive Formations:

One of the main challenges during the drilling of deep HPHT wells is the low rate of penetration. Nearly half of the rig time may be spent drilling the last few hundred meters. The slow advancement rate (1 to 2 m/h), along with excessive tool wear, is mainly due to the abrasiveness of the formations and the high compressive strength of the reservoir rocks.

I.5.2) Well Control:

Well control is a major concern in HPHT drilling operations, primarily due to the high frequency of influxes. Several factors contribute to this issue:

➤ **Extremely Narrow Mud Weight Window:**

In HPHT formations, pore pressure often lies just below the fracture gradient, so the allowable equivalent mud weight window can be on the order of only 0.02–0.05 sg; exceeding it by even 0.01 sg risks fracturing the formation and losing mud, while dropping below it invites formation fluids into the wellbore (kicks).

➤ **Wellbore “Pistoning” (Breathing) Effects:**

Cyclic pump in/pump out operations cause the borehole walls to elastically expand under pressure and then contract when circulation stops, creating transient volume changes (“pistoning”) that can mask true losses or gains and confuse surface indicators.

➤ **False Kick Indicators from Temperature Driven Mud Expansion:**

Elevated bottom-hole temperatures (often > 400 °F) cause oil-based mud to thermally expand downhole; when that expanded volume returns to surface, it can mimic an influx—triggering false kick alarms.

➤ **Hole Ballooning Due to Wellbore Elasticity:**

Under continuous circulation, the annulus pressurizes and wellbore walls balloon outward; upon shut-in, they rebound and expel excess mud. This “hole ballooning” leads to overestimation of returns and can conceal small influxes.

➤ Gas Liberation from Oil-Based Mud:

Dissolved gases (methane, H₂S) held in solution by high pressures and temperatures come out of solution when pressure or temperature drops—reducing the effective hydrostatic head of the mud column and risking unrecognized kicks[2].

I.5.3) Pressure Challenges:

The difficulties of downhole pressure, particularly pore pressure—the force imposed by fluids trapped within the pores of reservoir rocks—are initially encountered by drillers. Because of the weight of the geological layers above, pore pressure rises as drilling depth increases (overburden). A pressure gradient that varies according to geological formations and structures causes this increase.

Engineers use weighted drilling fluids to keep formation fluids out of the wellbore. The pore pressure of the formation is offset by the hydrostatic pressure produced by these fluids. To ensure wellbore stability and safety, precise pore pressure forecast prior to drilling is crucial.

The hydrostatic gradient of seawater is frequently used by engineers to determine "normal" pore pressure. However, many formations require drilling fluids with densities far higher than seawater because of their complex geology and changing overburden. In actuality, mud weights more than twice as large as seawater are commonly used while drilling high-pressure wells. Notably, even at very shallow depths, over pressured formations—with higher-than-normal pore pressure—can arise.

Hydrostatic pressures in contemporary ultra-deep wells, which can reach depths of up to 10,700 meters (35,000 feet), can surpass 207 MPa (30,000 psi). All well components, including drilling assemblies, LWD tools, wireline tools, completion systems, and intervention equipment, face considerable challenges as a result of this tremendous pressure.

Engineers place a strong emphasis on sealing systems and sophisticated materials to survive such circumstances. High-performance metals and alloys from the nuclear and aerospace industries have been incorporated into the oil and gas business. However,

Chapter I : The HPHT wells and gauges

the application of these materials is limited by wellbore space, particularly in deep water conditions. Tools used in such confined areas need to be tiny enough to pass through narrow wellbore diameters and able to withstand high temperatures and pressures. Sealing components must withstand high temperatures and pressure cycles repeatedly without failing.

Risks associated with pressure are not limited to downhole equipment. Employee safety is at danger due to high surface pressures during completion, testing, and production. All subsurface and surface systems must be built to function above the maximum anticipated pressure in order to counteract this. The component with the lowest rating in the pressure control equipment string determines the overall system rating.

Strict criteria must be followed when choosing and designing pressure control equipment. The expected maximum pressure is used to determine component selection, which affects sealing mechanisms, material thickness, elastomer arrangement, and pressure barriers. To guarantee safety and dependability during field operations, equipment must be function tested at pressures higher than anticipated operating conditions before to deployment.

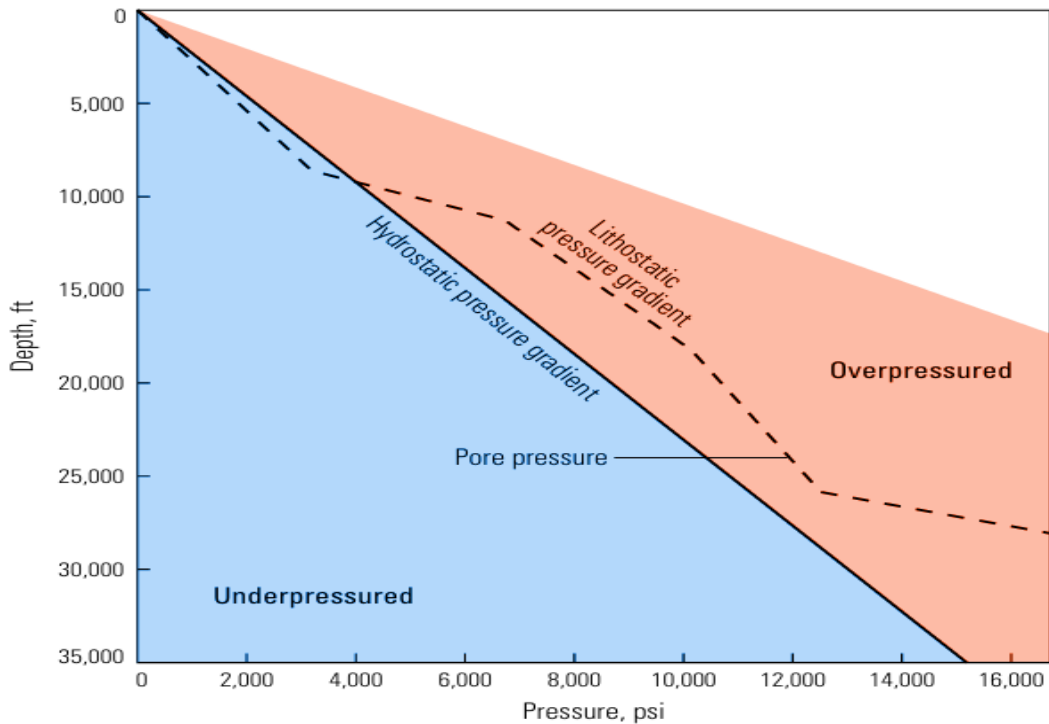


Figure I.3: Pressure gradients. The hydrostatic pressure gradient (black line), assuming seawater, is 0.43 psi/ft [9.79 kPa/m]; it follows a straight line [3].

The lithostatic pressure gradient (dashed black line) represents the actual downhole pore pressure and is a product of fluid, overburden and abnormal pressures; it can change across geologic features such as faults and depleted reservoir zones. Underpressured reservoirs (blue) have pressure below the hydrostatic gradient; overpressured conditions (pink) have pressures above the hydrostatic gradient [3].

I.5.4) Temperature Challenges:

Due to the average Earth's geothermal gradient of 1.4°F every 100 feet (2.55°C per 100 meters), drilling deeper than 19,700 feet (6,000 meters) is usually necessary to achieve 350°F. However, because of operational activity or naturally occurring geothermal hotspots, downhole temperatures can vary greatly. For instance, steam injection for heavy oil recovery in shallow wells may significantly raise temperatures, whereas deepwater wells frequently have smaller gradients and might not approach high-temperature thresholds even if they are deep.

Chapter I : The HPHT wells and gauges

The equipment and the operation used will determine how high temperatures are mitigated. The operating duration of Wireline and Logging While Drilling (LWD) equipment is limited by the use of high-temperature electronics and, occasionally, protective Dewar flasks. Temperature-resistant elastomers are also used by tools to seal in harsh environments.

Because the bottomhole assembly's (BHA) constant drilling fluid circulation helps regulate tool temperature, LWD tools often have lower temperature tolerance than wireline tools. Drilling fluids are occasionally pre-cooled to safeguard components that are susceptible to heat.

High-temperature drilling usually uses oil-based mud (OBM) systems because certain OBMs retain their characteristics at high temperatures. OBMs, on the other hand, retain heat better than water-based systems, which frequently leads to greater downhole tool temperatures and more thermal exposure [4].

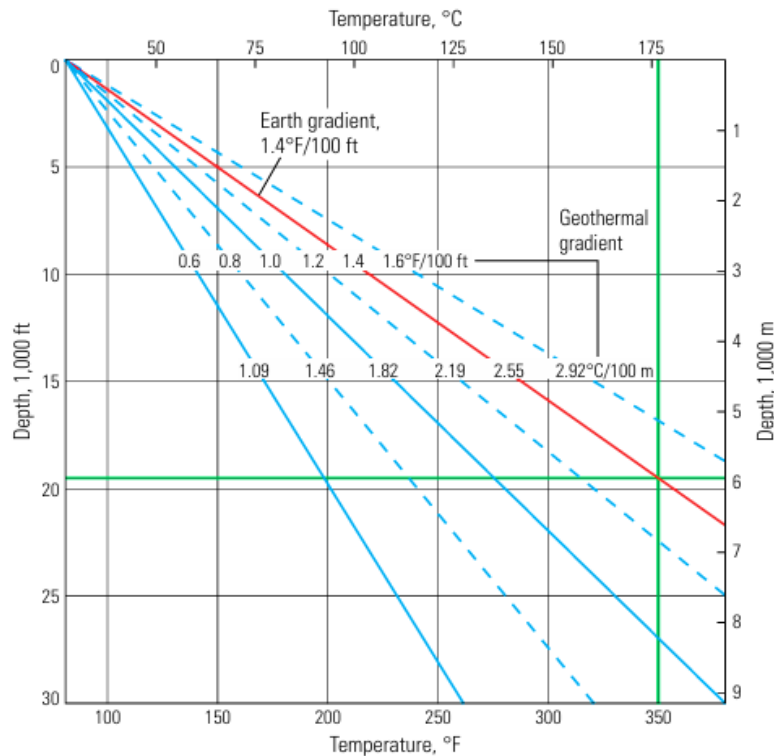


Figure I.4: Earth's geothermal gradient [3].

Chapter I : The HPHT wells and gauges

To reach the HPHT threshold of 350°F (vertical green line) and Earth's average geothermal gradient of 1.4°F/100 ft (red line), a well would have a depth of almost 20,000 ft [6,100 m] (horizontal green line). The thermal gradient will vary based on subsurface conditions and is not usually linear as shown.

I.6) Oil & Gas Well Types:

I.6.1) Exploration Wells (Wildcat Wells):

These are the first wells drilled in a new area to discover hydrocarbons. Often located in unproven regions, they carry a high risk of failure but potentially offer huge rewards. They may also be used to extend the boundaries of known reservoirs. It typically takes up to five years from discovery to production.

I.6.2) Appraisal Wells:

Once a discovery is made, appraisal wells are drilled to determine the size, potential production rate, and viability of a reservoir. They are more expensive than exploration wells but offer better chances of success and are critical for planning development.

I.6.3) Development Wells:

After confirming a discovery's viability, development wells are drilled for production. These are the most reliable and expensive wells, aiming to maximize output based on prior data. They are crucial for the efficient and economical extraction of oil and gas from known reserves.

I.6.4) Other types of wells:

- **Sidetrack Wells:** Drilled from an existing well to bypass a blockage or target a new zone if the original path is no longer viable or depleted.
- **Relief Wells:** Used to control blowouts or leaks in damaged wells by intersecting them at depth and injecting materials to stop the flow.
- **Injection Wells:** Inject fluids (e.g., water, CO₂) into underground formations to enhance recovery, store waste, or prevent saltwater intrusion.

Chapter I : The HPHT wells and gauges

➤ **Horizontal Wells:** Extend horizontally after reaching depth, allowing greater access to the reservoir. Frequently used with hydraulic fracturing (fracking), which injects high-pressure fluids to fracture rock and release trapped hydrocarbons.

I.7) Drilling Techniques:

- **Vertical Drilling:** The traditional method where the well is drilled straight down.
- **Horizontal Drilling:** Allows the drill to turn laterally to reach wider or more complex reservoirs, often improving recovery and efficiency [5].

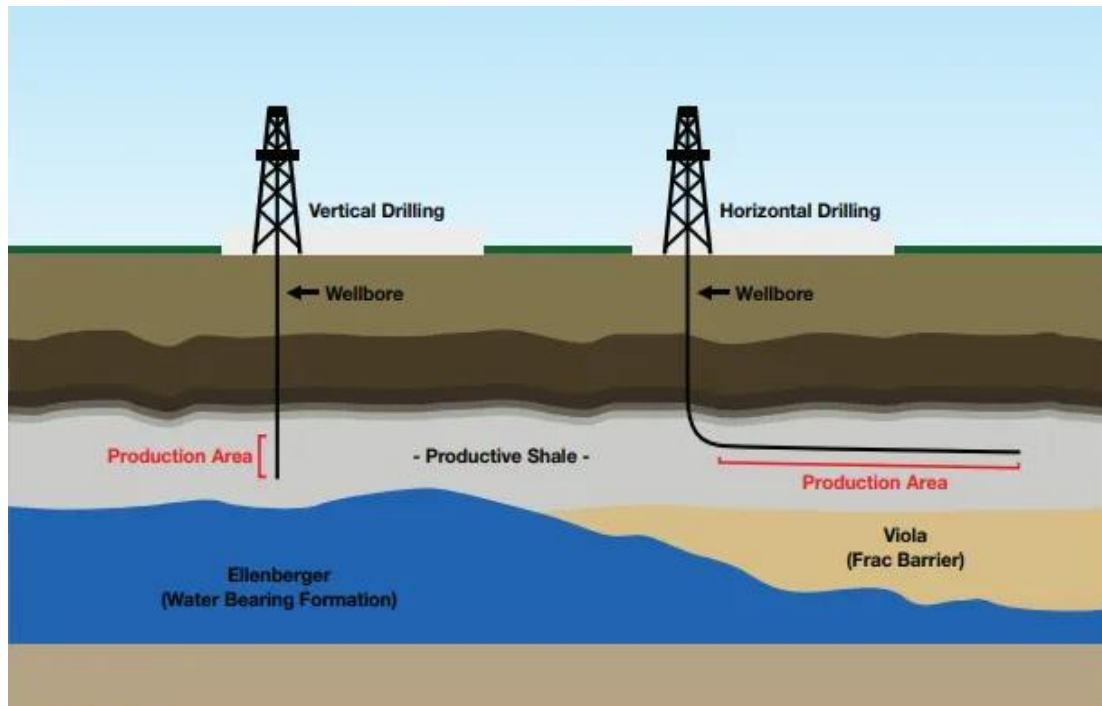


Figure I.5: vertical and horizontal drilling [5].

I.8) Steps And Phases For Drilling Oil And Gas Wells:

This high-level overview summarizes the principal stages in bringing an oil or gas well from concept to abandonment.

I.8.1) Planning & Preparation:

➤ **Site Selection:** Interpret seismic, geological and geophysical data to pick a subsurface target and a feasible surface pad location.

Chapter I : The HPHT wells and gauges

- **Permitting & Compliance:** Secure all environmental, safety and regulatory approvals.
- **Well Design:** Define the well path, casing program and drilling fluids plan whether vertical, directional, horizontal, multilateral or extended-reach.

I.8.2) Mobilization:

- **Rig Selection:** Match the well requirements to a suitable land or offshore rig, either from your fleet or via contract.
- **Pad Build & Move-In:** Clear and grade the site, construct roads and install utilities, then transport and position the rig modules.

I.8.3) Spud & Conductor Installation:

- **Spudding:** Drill the initial surface hole to establish a starting point.
- **Conductor Pipe:** Set and cement the large-diameter conductor string to stabilize the top of the borehole.

I.8.4) Surface-Hole Drilling:

- **Drilling:** Advance to the first casing depth (typically a few hundred meters).
- **Surface Casing:** Run and cement to isolate shallow aquifers and loose formations.
- **Circulation & Stability:** Treat any mud losses with lost-circulation materials or mud-weight adjustments; shore up unstable sections by fine-tuning fluid density.

I.8.5) Intermediate-Hole Drilling:

- **Drilling:** Continue drilling to the next pre-set casing depth, passing through varying formations.
- **Intermediate Casing:** Run and cement one or more strings or liners to seal off troublesome zones.
- **Directional Control:** Deploy down-hole motors, stabilizers or rotary-steerable systems to keep on the planned trajectory.

I.8.6) Production-Hole Drilling:

- **Drill to Total Depth (TD):** Reach the reservoir target.

Chapter I : The HPHT wells and gauges

- **Open-Hole Logging:** Conduct wireline or tubing-conveyed logs to evaluate formation properties and hydrocarbon presence.
- **Production Casing/Liner:** Install and cement the final production string (or leave as an open hole with a slotted liner, if specified).

I.8.7) Completion Operations:

- **Perforating:** Run perforation guns (via wireline or tubing) to create paths for reservoir fluids.
- **Stimulation:** Perform acidizing or hydraulic fracturing to boost well flow.
- **Completion Equipment:** Set packers, install tubing and other down-hole hardware.

I.8.8) Testing & Evaluation:

- **Well Testing:** Flow the well to surface, recording pressures and flow rates.
- **Data Analysis:** Interpret test results to estimate reservoir performance and economic viability.

I.8.9) Production Start-Up:

- **First Flow:** Open the well for sustained production.
- **Surface Facilities:** Commission separators, storage tanks and pipelines for handling and transport.

I.8.10) Monitoring & Maintenance:

- **Surveillance:** Continuously track production data and well integrity.
- **Workovers:** Perform remedial operations as needed to maintain or enhance output.

I.8.11) Plugging & Abandonment (P&A):

- **P&A Planning:** Design a safe, compliant abandonment program when the well is depleted or no longer economic.
- **Execution:** Set cement plugs, remove equipment and restore the site to agreed standards. [6]

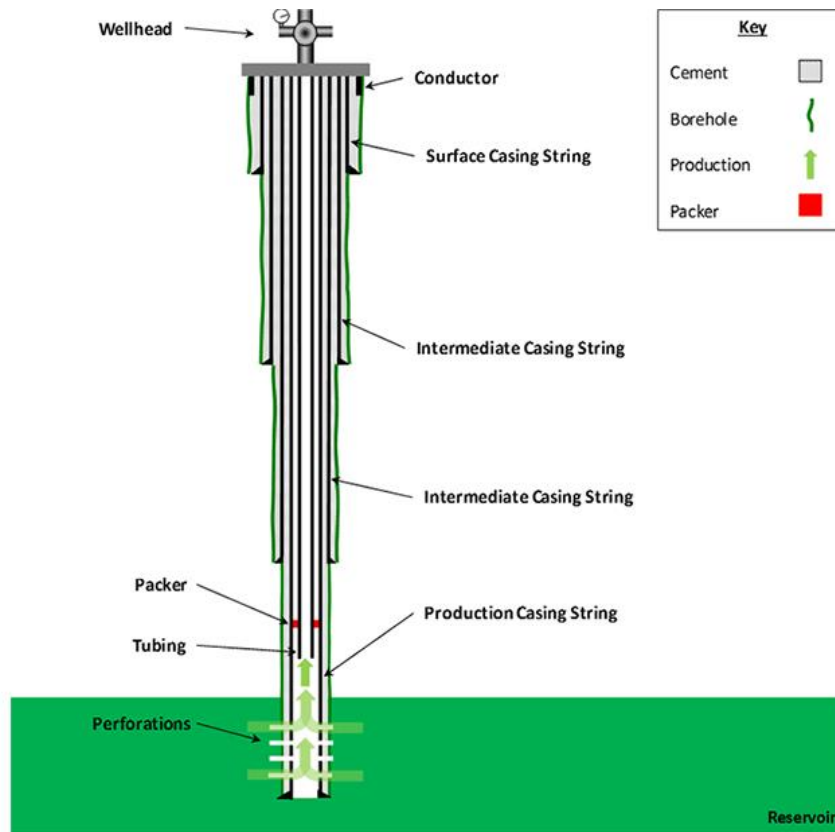


Figure I.6: Typical Hydrocarbon Production Well with Multiple Casing Strings including two Intermediate Casing Strings [7]

I.9) Downhole Gauges:

Downhole gauges are advanced instruments specifically engineered to monitor vital parameters within a wellbore. These tools are deployed directly into the well, enabling them to collect real-time data from the reservoir environment. The most commonly measured parameters include:

- **Pressure:** Gauging the pressure exerted by fluids in the reservoir, which provides insights into pressure gradients, well productivity, and potential risks such as fracturing.
- **Temperature:** Tracking the temperature of reservoir fluids to detect thermal anomalies, determine fluid properties, and identify risks like gas hydrate formation.

Chapter I : The HPHT wells and gauges

- **Flow Rate:** Measuring the volume of fluids moving through the wellbore, offering critical data on production rates, well performance, and potential bottlenecks.

I.9.1) The Importance of Downhole Gauges:

Downhole gauges deliver several key benefits to oil and gas operations, including:

- **Optimized Production:** Accurate data allows operators to identify flow restrictions, fine-tune flow rates, and develop efficient production strategies.
- **Improved Reservoir Management:** Understanding pressure, temperature, and fluid dynamics enables informed decisions on reservoir depletion, injection planning, and overall management.
- **Enhanced Safety and Risk Mitigation:** Constant monitoring of critical parameters helps detect threats like wellbore instability, gas leaks, or formation failure early, enabling timely intervention and accident prevention.
- **Real-Time Monitoring and Data Acquisition:** These gauges offer continuous reservoir monitoring, allowing operators to respond rapidly to changes and optimize performance in real-time. [8]

I.9.2) Pressure and temperature gages:

An electronic gauge that gauges the temperature and pressure inside the tube serves as the sensing element. A mandrel, which is a component of the tubing string, holds the gauge in place [9].

In a variety of applications, the downhole instrument may measure downhole parameters including temperature, pressure, and flow rates, providing useful information to reservoirs and producing gas, water, producer, or injector wells [10].

I.10) Type of gauges:

I.10.1) Quartz Crystal Gauges:

Quartz crystal gauges employ piezoelectric quartz crystals to measure downhole pressure and temperature in high-pressure, high-temperature (HPHT) wells. They withstand pressures up to 30 000 psi and temperatures exceeding 437 °F (225 °C) [12]. Their high-resolution capability—detecting pressure differences as low as 0.005

Chapter I : The HPHT wells and gauges

psi—makes them indispensable for reservoir diagnostics and real-time monitoring in hostile environments [12]. For example, Schlumberger’s Signature Quartz Gauge integrates an all-ceramic, single-substrate multichip module with proprietary wireless telemetry to optimize data accuracy and reliability in HPHT wells [12, 3].

I.10.2) Sapphire/Piezoresistive Gauges:

Sapphire-based piezoresistive gauges utilize silicon-on-insulator (SOI) technology and electron-beam-welded housings to enhance durability in corrosive, sour-gas, and geothermal applications. These sensors are rated for pressures up to 30 000 psi and temperatures up to 437 °F (225 °C), making them suitable for Level II and III HPHT operations [11, 9].

I.10.3) Permanent Downhole Monitoring Systems:

Permanent downhole monitoring systems integrate bidirectional telemetry (e.g., FDMA) and corrosion-resistant materials to deliver continuous real-time data for long-term reservoir management. Schlumberger’s Metris™ systems, for instance, are engineered for operational lifetimes exceeding 20 years at 400 °F (204 °C) and feature redundant sensors to mitigate risks in ultra-deep wells [9].

I.10.4) Memory Gauges:

Memory gauges record pressure and temperature data for post-retrieval analysis. Electronic Memory Recorders deployed via slickline or coiled tubing in HPHT well testing are rated for pressures up to 30 000 psi and temperatures up to 392 °F (200 °C) [18]. Their compact design and high-capacity memory modules enable detailed pressure-transient analyses in challenging downhole environments [13].

I.10.5) Signature quartz gauge:

The tool is rated for use in extreme environments, with a temperature tolerance of up to 437°F (225°C) and a pressure rating of up to 30,000 psi (207 MPa). Downhole reservoir testing, exploration or appraisal testing, HPHT (high-pressure, high-temperature) wells, hostile and extreme-temperature environments, and pressure surveys in production wells are just a few of the difficult applications for which it is made. Both memory mode testing and wireless readout are supported. The instrument

Chapter I : The HPHT wells and gauges

increases operational precision and confidence by providing dependable performance in HPHT situations. By enhancing reservoir description, it also reduces risk, which eventually aids in improved decision-making and well optimization.[12]

➤ **The way it functions :**

Cutting-edge technology are included into the Signature* quartz gauge to reliably deliver the best pressure readings in any setting. With increased precision, high-resolution measurements are taken to better quantify reservoir characteristics, allowing for testing to be done with confidence throughout the field's lifespan. The Signature gauge has the highest temperature rating available and is made for the harshest downhole conditions. The gauge, which is rated to 30,000 psi and 437 degF, provides accurate readings that allow the operator to look beyond the area close to the wellbore, recognize intricate reservoir characteristics, and spot even small pressure variations that can have a big impact on field development plans.

The Signature gauge's all-ceramic, single-substrate-constructed multichip module (MCM) and proprietary electronics for exceptional resolution and efficient operation combine to provide resolution that can detect pressure differences of less than 0.005 psi at a 1-s recording rate, enabling analysis that was previously unfeasible. Because there are fewer connections and components when the electronics with 100% ceramic MCM components are placed onto a single substrate, dependability is increased under harsh downhole circumstances. Additionally, the ceramic substrate guarantees that electronics will last a long time at high temperatures. To make sure the gauge has the finest power supply possible, Schlumberger battery professionals also design, construct, and test batteries.

The QuarteZ downhole reservoir testing equipment uses the Signature gauge to monitor test progress at high frequencies. With the use of wireless telemetry, the gauge can provide real-time pressure readings for thorough downhole test progress tracking. It is possible to query each gauge separately for current or past temperature or pressure readings [12] .



Figure I.7: Signature gauge.[12]

➤ **Hybrid Systems with SOI Electronics:**

Hybrid systems combine quartz sensing elements with SOI electronics to address extreme HPHT conditions. Emerson's Roxar HS Series, designed for subsea applications, employs multi-drop connectivity to monitor annulus pressure and reservoir performance in real time [14]. Such systems are critical for Level III HPHT operations, where temperatures can exceed 500 °F (260 °C) and pressures may reach 40 000 psi [2].



Figure I.8: Quartz Memory Tool gauge [11]

I.11) Conclusion:

Exploring and producing High Pressure High Temperature (HPHT) wells presents significant challenges due to extreme subsurface conditions. Success in these operations relies on precise modeling, real-time monitoring, advanced sealing, and adaptable design standards. Accurate knowledge of pressure and temperature is essential for optimizing production, preventing failures, enhancing pump performance, and selecting effective enhanced oil recovery (EOR) methods. These data also play a vital role in reservoir analysis and forecasting, enabling engineers to understand reservoir behavior, identify fluid types, and plan long-term, efficient extraction strategies. Future advancements in materials, telemetry, and sensors promise even safer and more sustainable HPHT operations.

Chapter II:

Data transmission

II.1) Introduction:

In the ever-evolving petroleum industry, one of the most technologically complex challenges is the transmission of real-time data from High Pressure High Temperature (HPHT) downhole gauges to the surface or remote monitoring systems. These gauges, designed to operate in extreme subsurface conditions, are essential for capturing critical parameters such as pressure, temperature, and fluid flow, which directly impact well performance, safety, and decision-making.

However, acquiring this data is only part of the process—the reliable transmission of information through kilometers of high-stress wellbore presents significant engineering hurdles. The harsh environment demands the use of high-temperature electronics, robust telemetry systems, and durable materials capable of withstanding thermal and mechanical stress.

Modern solutions include wired and wireless telemetry, acoustic or electromagnetic signals, and increasingly, satellite-linked systems for global data access. This chapter explores the principles, challenges, and cutting-edge technologies behind downhole data transmission, emphasizing its vital role in real-time reservoir monitoring, production optimization, and the future of intelligent oilfield operations.

II.2) Wire communication downhole data:

II.2.1) Traditionally Wireline logging:

Traditionally Wireline logging tools are rated for continuous operation to 350°F and 20,000 psi downhole conditions. With many reservoirs exceeding these limits, the need for specialized, High-Pressure and/or High-Temperature Wireline tools has been an issue for some time. Sensors were accordingly developed to ratings of 500°F and 25,000 psi. Recently, Ultra-Deep drilling has pushed the boundary to above 25,000 psi, resulting in the development of 30,000 psi and 500°F rated wireline tools. Currently, basic Petrophysical evaluation Quad-combo strings are available and wells in excess of 480°F, 26,000 psi have been successfully evaluated [13].

II.2.2) Wired Pipe line:

The measured data from sensors on top of the bit and the data from sensors along the drill string are sent to the surface in real-time during drilling using intelligent drill pipe telemetry[14]

The wired pipe system is made up of a wireless surface interface system, a downhole interface sub, and the wired pipe string. [15]

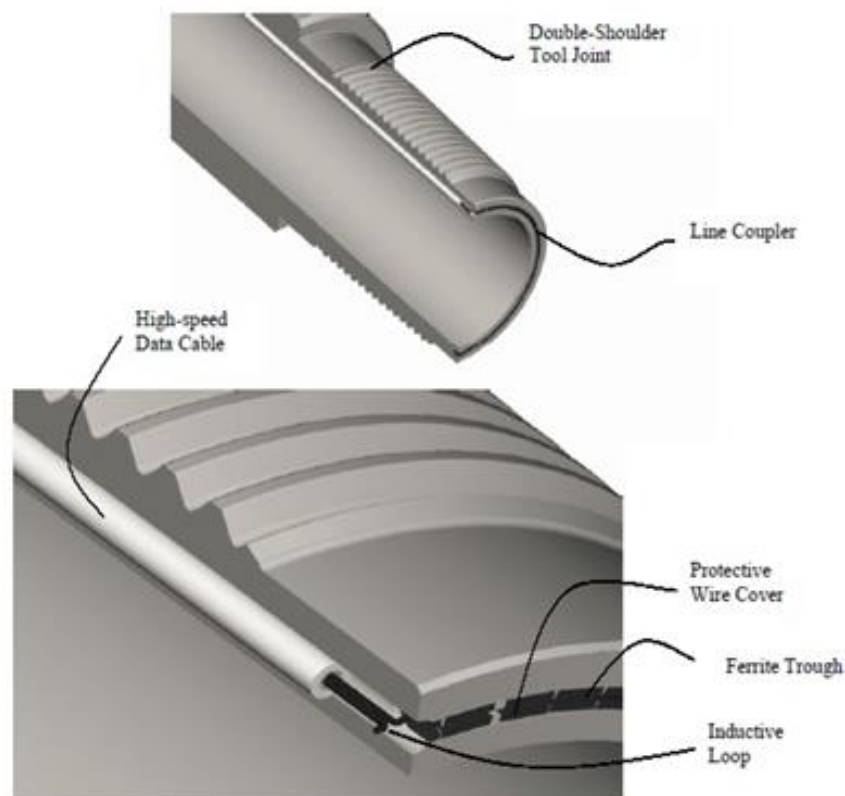


Figure II.1: Cutaway view of the telemetry drill pipe system in a drill pipe connection [15].

➤ Technological description

A passive communications link that joins disparate parts is the fundamental technology of the telemetry drill pipe system. This link consists of a high-speed data wire that runs the whole length of each drill pipe segment and is enclosed in a stainless steel tube that is pressure-sealed. In order to keep the conduit against the

Chapter II: Data transmission

tube wall and minimize interference with mudflow or tools in the pipe center, it is maintained under tension within the drill pipe tube.

At the internal upset, the conduit enters the drill pipe's internal diameter after passing through the tool joint's body. The cable transmits data across each tool joint contact and ends at inductive coils that are positioned in the pin nose and matching box shoulder of each connection (Reeves et al., 2005). Figure 8 provides an illustration of this idea.

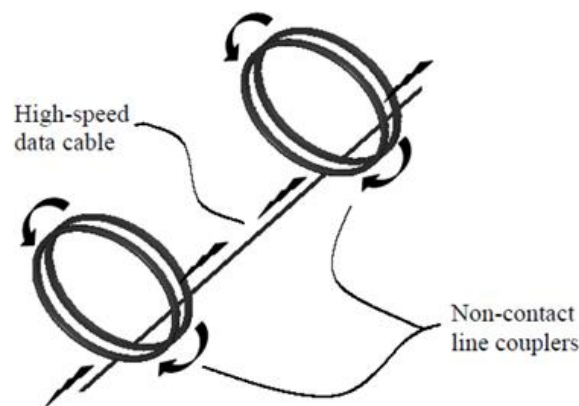


Figure II.2: The non-contact line coupler uses induction to transmit data from one connection to another [15].

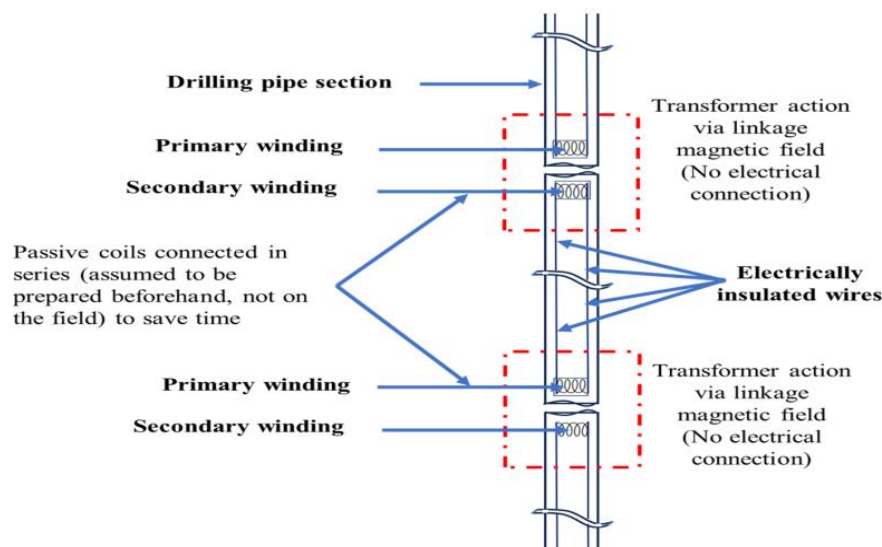


Figure II.3: Data transmission concept by using intelligent drill pipe telemetry [14].

Chapter II: Data transmission

II.2.3) Optic fibry transmission :

Permanent downhole installation and dependable pressure and temperature acquisition, even under high pressure, high temperature (HPHT) circumstances, are features of the Fibre Optic Well Monitoring (FOWM) system. FOWM is based on an optical sensor system idea that combines fiber optic communication with basic passive silicon resonator sensors [15].

Real-time, high data rate transmission is made possible via fiber optic connection as opposed to conventional downhole transmission techniques. But the main issue facing downhole optical communication is how to guarantee extended functioning in the hostile environment, which is marked by high pressures, high temperatures, and corrosive materials[17] .

II.3) Wireless communication downhole data:

With this novel method, downhole data may be electronically delivered without the need for a wireline. For both open and cased holes, the method involves low frequency electromagnetic transmission through the formation. As sending and receiving devices, two antennas are employed, one downhole and one at the surface. The DST string contains the downhole antennas, which form the dipole by means of an insulating gap. The method depends on the formation's resistivity since the higher the resistivity, the more the signal dissipates. The method is only effective in specific operational settings [18]

II.3.1) Electromagnetic Telemetry:

The 1980s saw the introduction of the electromagnetic telemetry (EMT) technology. It is comprised of a transmitter that uses an implanted electrical insulating layer (the transmitter) to transfer data via coded electromagnetic waves. This installation is made feasible by the drill string's usage as a dipole electrode, which creates an altered voltage differential. The channel or propagation medium that uses the formation (which is) next to the wellbore makes up the remaining communication components. The data is sent to the receiver as a measured voltage differential between the wellhead and an antenna that is fixed to the ground. For operation, a casing antenna may be added in addition to the system. [19] , As distinct expressions

Chapter II: Data transmission

of the same event, electric and magnetic fields combine to form electromagnetic fields. [20]

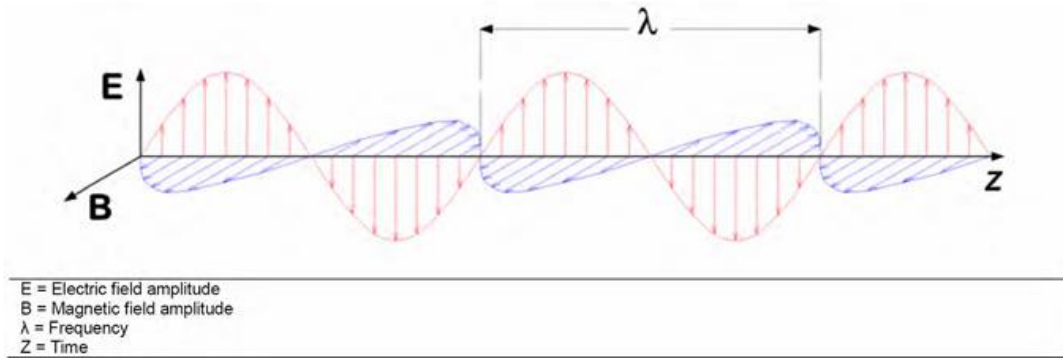


Figure II.4: Electromagnetic Waves [19] .

➤ **Electromagnetic communication principle:**

Faraday's Law of Induction rules the EM coupling communication.

$$\oint \mathbf{E} \cdot d\mathbf{l} = -\frac{d\phi_B}{dt} \quad (\text{II.1})$$

In difficult downhole conditions including high-pressure/high-temperature (HPHT), sour and caustic conductive liquids, and others, it has a significant anti-jamming capacity. The magnetic field is non-propagating and largely a diffusion field in a conductive material because an AC magnetic-dipole field produced by electromagnetic coupling in the radio frequency spectrum is a near field with little or no electric field. Coaxial hollow solenoids of similar length make up inductive coils. Therefore, in order to transmit a signal, the theory mathematical model of EM coupling communication between input and output is given by :

$$\varepsilon_2 = \pm K\sqrt{E^2 - \varepsilon_1} \quad (\text{II.2})$$

Where:

$$K = -\frac{\pi^2 n_1}{2\alpha_1 n_2} \left(\frac{d_1}{l}\right)^2 \left(\sqrt{1 + 4\left(\frac{l}{d_2}\right)^2} - 1\right) \quad (\text{II.3})$$

Chapter II: Data transmission

(n_1 , n_2 , d_1 and d_2 are the number of turns and diameter for stimulated coils and inductive coils respectively. l is the length of coils), α_1 is related with l/d_1 , ϵ_1 is stimulated voltage, ϵ_2 is inductive voltage, and E is the amplitude of signal. [20]

Extremely Low Frequency waves, or ELF, are used in downhole electromagnetic telemetry for a number of reasons, including unguided waves, vast transmission distances, and conductive and heterogeneous substrates.

Since all of these elements contribute to the overall attenuation, the frequency is lowered as much as possible, usually between 0.1 and 20 Hz, and the range is restricted to 500–3000 meters. Multiple electromagnetic devices can be utilized at regular intervals to receive and retransmit the signals when longer distances need to be covered. These extra devices, known as repeaters, raise the system's cost and complexity while lowering its dependability. Figure II.5 below depicts a typical EM wireless telemetry system.

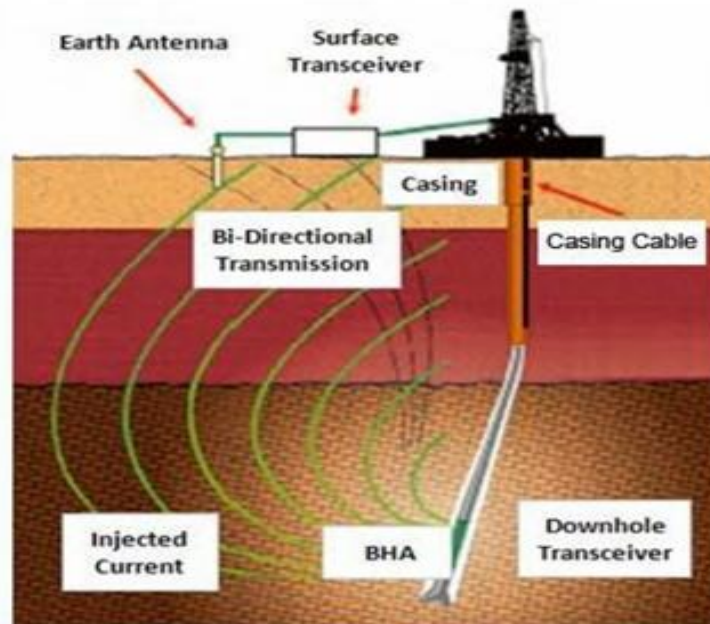


Figure II.5: Example of electromagnetic telemetry in a well [20]

The ability of EM telemetry to pass through the formation and, more effectively, via wellbore tubulars is a significant benefit. Typically, the signal is obtained by detecting the time-varying electric, magnetic, or current fields between the tubing's surface and an earth antenna, or grounding rod, buried far from the wellhead. [20]

Chapter II: Data transmission

II.2.2) Acoustic wave:

Operating on batteries, the acoustic telemetry system is unique from previous systems in that it uses sonic waves to send real-time data to the surface through pipe walls up to 12,000 [ft.]. Pressure, temperature, time, commands, and system status information are just a few of the many types of data that may be obtained and sent. The primary applications for this telemetry system are well-testing procedures and exploratory wells. Just above the tester valve, meters with quartz crystal sensors produce precise temperature and pressure readings in the deep end that can either be sent straight to the surface or retained in recording memory, . There is a significant deal of versatility because each quartz sensor can retain up to 440,000 readings in its memory, and the system as a whole can store over 1.3 million scans [22] .

a) Principle of Acoustic wave:

The Acoustic Telemetry Principle By encoding data into elastic (acoustic) waves that travel down the drill string or via the drilling fluid as a waveguide, acoustic telemetry delivers downhole measurement data. Digital data is represented by pressure pulses or torsional waves produced by a downhole transmitter, usually a piezoelectric or magnetostrictive transducer, at certain carrier frequencies (usually in the 700–2000 Hz range) [23]. These guided waves undergo frequency-dependent attenuation and dispersion as they ascend the drill string, as explained by:

$$A(x) = A_0 e^{-\alpha x} \quad (\text{II.3})$$

where $A(x)$ is the wave amplitude after distance x , and α is an attenuation coefficient that relies on the fluid coupling and pipe material and rises with the square of frequency [25]. These waves are picked up at the surface by sensitive receivers (collar-mounted transducers or clamp-on hydrophones); the original bits stream is recovered by sophisticated signal processing (convolutional decoding, matched filtering) [23].

b) Components and Operation:

➤ **Downhole Transmitter:** An electroacoustic transducer that transforms electrical telemetry signals into guided waves. It can be either

Chapter II: Data transmission

Gigantic magnetostrictive or piezoelectric. Low-frequency output and high-temperature robustness are given priority in designs

The bit and transmitter are separated by a mechanical filter called an acoustic isolator, which reduces drilling noise (below 600 Hz) and stops uplink signal reflections, improving channel fidelity [24].

➤ **Waveguide (Drill String):** By choosing carrier frequencies within guided-wave passbands, which are supported by the drill-pipe periodic structure, distance and data rate are maximized [17].

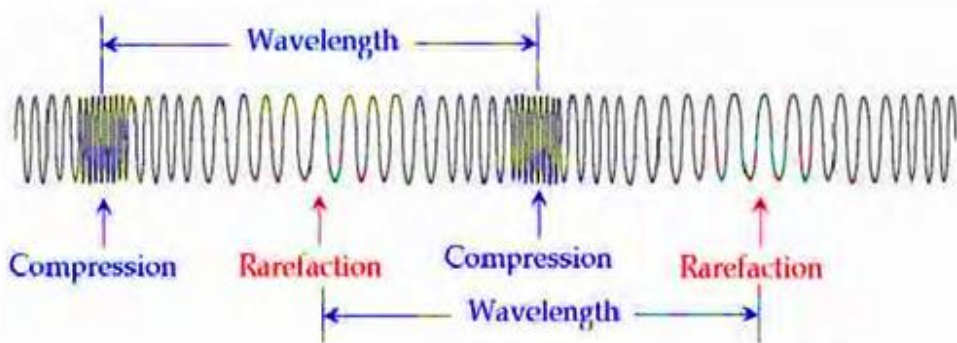


Figure II.6: Longitudinal waves in a spring are a good analogy for compressional acoustic waves in the tubing string of a well [20].

➤ **Surface Receiver:** An integrated sensor assembly or clamp-on device that converts incoming auditory signals into digital data by filtering, amplifying, and decoding them [24].

Attenuation and Dispersion Attenuation in acoustic telemetry is predominantly because of fluid loading, dispersion at pipe connections, and viscous damping. The coefficient usually rises strongly with frequency ($\alpha \propto f^2$) and varies from 0.1 to 1 dB/m at 1 kHz. Drill-string modal analysis may forecast dispersion, a frequency-dependent phase velocity, which can deform pulse forms [27].

Chapter II: Data transmission

c) Schemes for Modulation Typical schemes include:

➤ **Frequency-Shift Keying (FSK):** Different digital symbols are represented by two or more carrier frequencies. Easy to implement yet susceptible to multipath-induced intersymbol interference [28].

➤ **Multipulse Block Encoding:** This technique improves the uniqueness of symbols and enables envelope-detection receivers to increase signal-to-noise ratios by combining sets of pulses with discrete time-amplitude patterns [25].

➤ **Phase-Shift Keying (PSK) and Orthogonal Multiplexing:** Less popular downhole because of issues with phase stability, but new studies indicate that they may have greater spectrum efficiency when paired with adaptive equalization and coherent receivers [26].

Data Rate and Range Advanced systems that use dual-frequency carriers and lock-in amplifiers have achieved error-free rates up to 64 bps at 2 km, while without repeaters, typical data rates are 1–10 bps across distances of 1–2 km [23]. Transmission distances above 5 km are possible with repeaters positioned 500–1,000,000 meters apart, but this comes with a higher cost and complexity to the system [26].

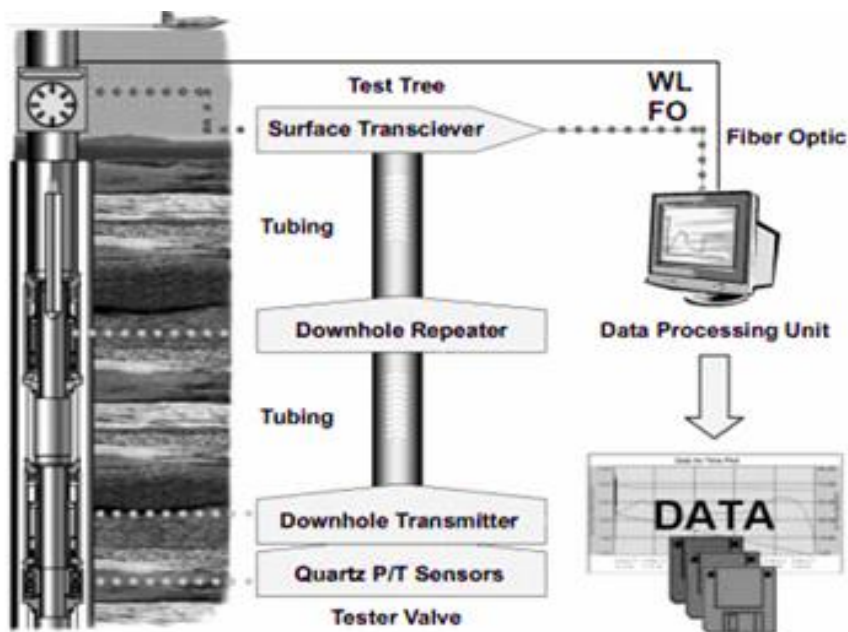


Figure II.7: Flow-chart of acoustic telemetry system operation [22]

Chapter II: Data transmission

II.2.3) Mud pulse telemetry (MPT) system:

This technology uses a module that adjusts the resistance to the drilling fluid flow through the drill string's interior, creating a rise and fall in the standpipe pressure and, consequently, mud pressure pulses that are indicative of the parameters determined by the logging tools and that travel to the surface roughly at the speed of sound. Surface-mounted transducers pick up the pressure signal and use analog/digital (A/D) converters to transform it into a digital electrical signal. After then, the signal is transmitted to a computer, which uses specially designed software to identify and handle the signal before processing and decoding it. [22]

a) Principle of Operation:

- **Pressure-pulse generation:** A downhole pulser (valve or “mud siren”) modulates the flow of drilling mud inside the drillstring to create discrete pressure disturbances—positive pulses (brief flow restriction), negative pulses (momentary flow bypass), or continuous-wave oscillations—each representing bits or symbols in a digital code [30].

- **Hydraulic waveguide :** The drilling fluid column transmits these pressure waves upward; its density and rheology govern wave speed ($\sim 1,300\text{--}1,500$ m/s) and attenuation [29].

- **Surface detection and decoding :** At the surface, a high-precision pressure transducer in the standpipe detects minute pressure variations. These electrical signals are filtered, digitized, and demodulated to recover the original downhole data stream .

b) Modulation and Data Encoding:

- **Binary on-off keying:** Early MPT systems encode a “1” by generating a pulse in a fixed time slot and a “0” by omitting it, forming simple on-off keying of pressure [32].

- **M-ary schemes:** To boost throughput, modern tools vary pulse amplitude, duration, or frequency—so called M-ary encoding—allowing multiple bits per pulse interval and effectively increasing data rates [30].

- **Telemetry frames :** Data are packetized into frames with preamble (synchronization), payload (sensor readings), and error-checking codes, typically transmitted every few seconds per frame [31].

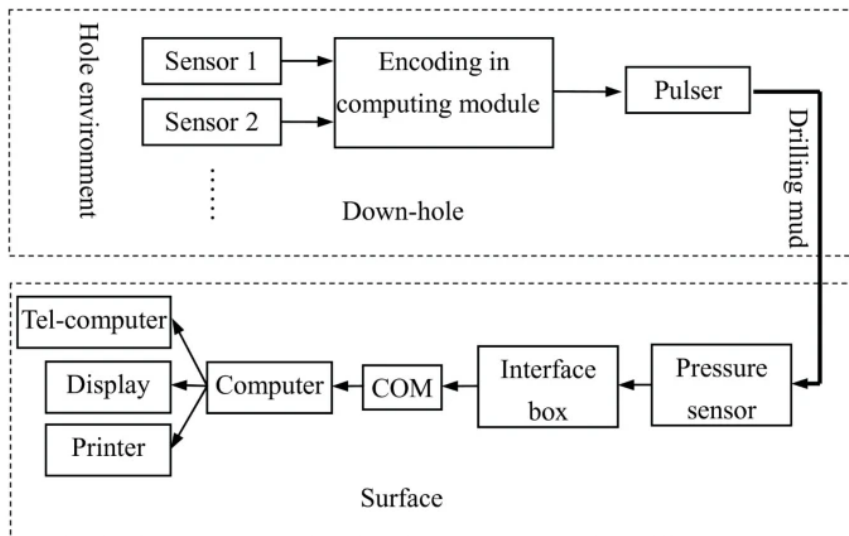


Figure II.8 : Signal flow of mud pulse telemetry [33]

II.2.4) Other Possible Downhole Telemetry Types:

Types Numerous researchers have examined wireless technology and offered ideas for new or current technologies to narrow the gap there are a number of other fundamental forms of energy, and various wireless telemetry features have been developed or suggested utilizing them:

- **Chemical telemetry:** is a type of digital telemetry that uses chemical tracers that are delivered downhole and continually monitored at the surface. Using separate timings, several tracers might be launched simultaneously, detected, and decoded at the surface. A system like this would be comparable to electromagnetic telemetry, which allows several frequencies to be sent concurrently over a single channel .One way to communicate wirelessly downhole is using

- **thermal telemetry:** The well fluid becomes closer to the formation's gradient temperature when the well is closed in. Both a DTS and a PDG can scan a thermal transient when the well is flowing and interpret it to determine the fluid type and flow rate. Longer flow durations reduce the effectiveness of this strategy because the near wellbore warms up and loses its ability to reflect the reservoir's gradient temperature. A PDG or other measurement tool in the well or at the surface is used to read the flowing temperature profile in HIPlog , an enhanced form of thermal telemetry that employs an autonomous heat source to produce a thermal pulse .

Chapter II: Data transmission

- **Nuclear telemetry** might be used similarly to the chemical telemetry mentioned above, however because of health, safety, and environment (HSE) concerns, even low order radioactive particles discharged freely in a moving fluid would not be appropriate [20].

II.4) Comparison of telemetry systems:

For each technology, data from various manufacturers were gathered, along with case studies and recent articles that reflect the latest advancements in each field, leading to a critical understanding. Electromagnetic telemetry is illustrated by Halliburton's Sperry Drilling EMT system; acoustic telemetry is represented by Halliburton's Acoustic Telemetry System (ATS); mud pulse telemetry is exemplified by Schlumberger's TeleSCOPE system integrated with the Orion II platform; and finally, wired drill pipe telemetry is depicted through the IntelliServ Network system developed by National Oilwell Varco..

Table II.1 offers a comparison of these telemetry systems in terms of transmission rates, maximum achievable depths, volume of transmitted data, and associated technology costs.

Table II.1: A comparative between different data transmission technologies [22].

Features	Telemetry Technologies			
	Electromagnetic	Acoustics	Mud pulses	Wire drill pipe
Transmission rate [bps]	10	20	120	57000
Maximum depth [ft]	18000	12000	40320	Unlimited
Data quantity	Medium	Low	High	Very high
Signal attenuation	High	High	Medium	N/A
Signal interference	High	Medium	Medium	Low
Costs	Medium	Medium	Low	High

Chapter II: Data transmission

An analysis of Table 1 reveals that for ultra-deep wells exceeding depths of 6000 meters, electromagnetic and acoustic telemetry technologies are unsuitable, mainly due to significant signal attenuation at such depths. Even with the implementation of signal repeaters, these methods remain limited to approximately 18,000 feet. In contrast, mud pulse telemetry and wired drill pipe telemetry continue to evolve technologically, consistently setting new depth records while maintaining highly efficient transmission rates.

A noteworthy observation is the significant disparity between the data transmission capacities of these technologies; however, this gap is somewhat offset by the high costs linked to wired drill pipe systems. Since the cost of wired drill pipes scales directly with well depth, their use is best reserved for high-value wells with guaranteed returns, making them less suitable for exploratory drilling. Consequently, mud pulse-based telemetry systems attract greater attention as the most viable option overall, enabling the acquisition of essential data at reasonable transmission rates.[22]

II.5) Future Development Trends:

As the oil and gas sector pivots toward smarter, more efficient and environmentally responsible operations, downhole electric bypass valve technology is advancing rapidly. Next-generation designs will emphasize intelligent automation, novel materials, enhanced energy performance, remote actuation, and resilience under extreme downhole conditions.

II.5.1) Leveraging AI and Big Data for Valve Management:

By embedding artificial intelligence and big-data analytics into downhole electric bypass systems, valve operation and oversight can be transformed. AI-powered control routines will process live well-bore data, forecast pressure swings and dynamically tweak valve positions to maximize output. Meanwhile, machine-learning algorithms will bolster anomaly detection—pinpointing early signs of wear or malfunction so that preventive maintenance can be scheduled and unplanned downtime minimized.

II.5.2) Harnessing 5G and IoT Connectivity:

Thanks to the rollout of 5G networks and the proliferation of IoT devices, operators will soon enjoy uninterrupted, low-latency access to downhole valve data.

Chapter II: Data transmission

High-bandwidth, cloud-based platforms will aggregate streams from numerous wells, delivering live performance metrics and alerts. This unified view empowers engineers to intervene instantly when anomalies arise and to fine-tune production parameters across their entire asset portfolio for maximum uptime and throughput

II.5.3) Diagnostics of Faults and Predictive Maintenance:

Real-time sensor data will be used by AI-driven predictive maintenance systems to identify wear and failure early on. Operators can improve reliability and decrease unplanned shutdowns by simulating valve performance under various situations by using digital twin technology [34].

II.6) Conclusion:

In the petroleum industry, reliable real-time data transmission from HPHT downhole environments is critical for operational efficiency, safety, and reservoir management. This chapter explored various wired and wireless telemetry systems, including traditional wireline logging, wired pipelines, fiber optics, electromagnetic, acoustic, and mud pulse technologies. Each method addresses unique challenges posed by extreme pressures, temperatures, and harsh downhole conditions. While wired systems offer robustness, wireless solutions like electromagnetic and acoustic telemetry provide flexibility but contend with signal attenuation and environmental interference. Emerging methods such as chemical and thermal telemetry present innovative alternatives, though practical limitations persist. Continuous advancements in materials, signal processing, and modulation schemes enhance data rates and transmission reliability. However, balancing technological complexity with operational feasibility remains a key consideration. As the industry progresses toward intelligent oilfields, integrating these evolving technologies will be pivotal in achieving real-time monitoring, optimizing production, and ensuring sustainable operations in increasingly challenging reservoirs.

Chapter III:
Simulation of HPHT Downhole
Wireless Telemetry

III.1) Introduction:

As we have laid the groundwork by defining HPHT well characteristics and surveying data transmission methods in the preceding chapters, Chapter III now transitions our focus to practical validation. This preamble frames an extensive MATLAB /Simulink simulation campaign designed to emulate the harsh downhole conditions of HPHT operations—pressures reaching 10 000 psi and temperatures up to 175 °. Here, we present the high-level modeling strategy: how theoretical signal pathways and encoding schemes are mapped onto computational constructs, the selection of performance metrics (signal integrity, propagation delay, bit-error rate, and overall reliability), and the criteria for comparing electromagnetic, acoustic, and mud-pulse approaches. By outlining the methodology, objectives, and evaluation framework, this section prepares readers for the detailed simulation results and analysis that follow, underscoring the indispensable role of virtual testing in guiding the design and optimization of robust downhole telemetry architectures.

III.2) Simulation of HPHT well telemetry in Real-time:

III.2.1) Electromagnetic wave using MATLAB:

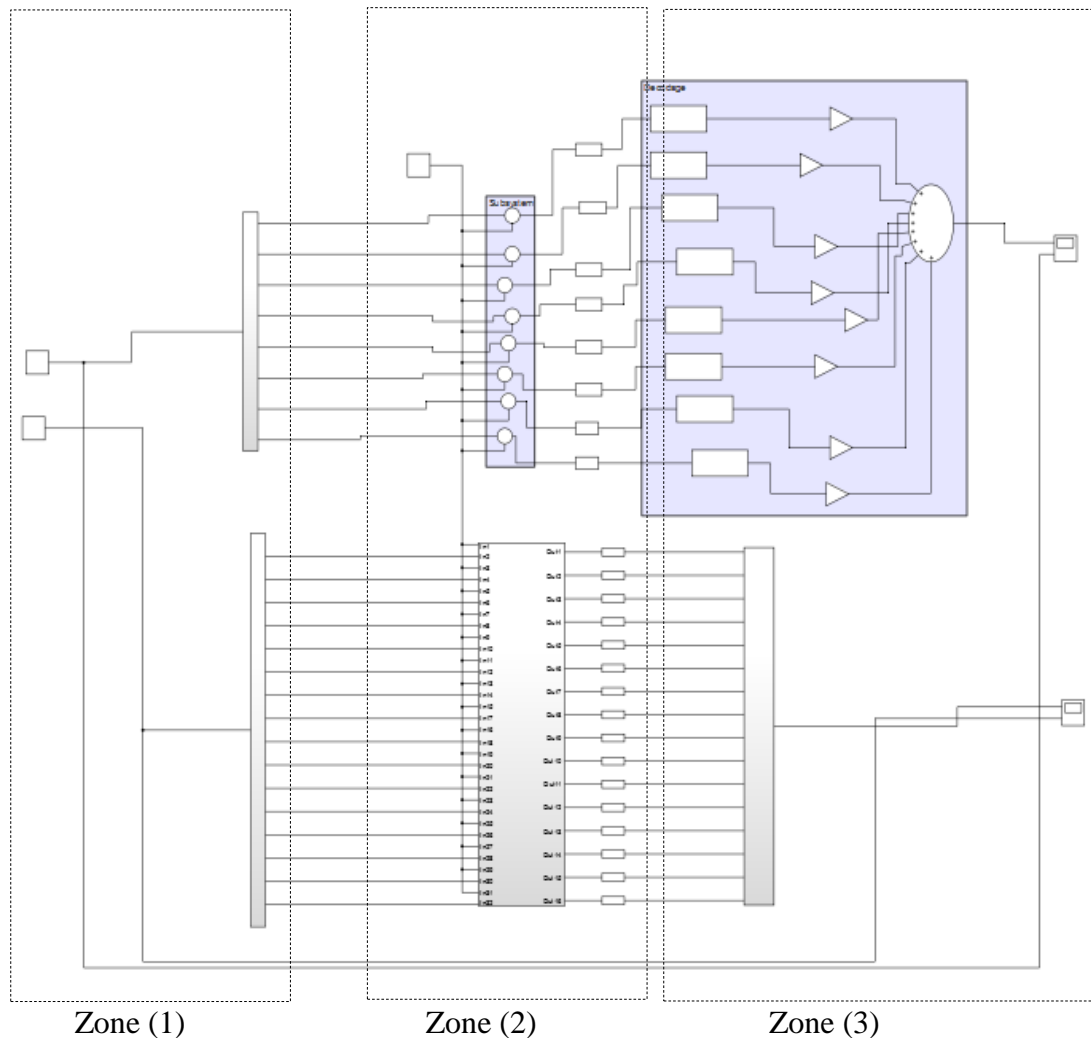


Figure III.1: Simulation of EM telemetry system using MATLAB

Zone(1): Downhole zone

Zone(2): Transmission zone

Zone(3): Workspace zone

➤ The first region, the downhole area, is where the sensor module is installed. This module comprises two primary sensors a temperature sensor and a pressure sensor each simulated in Simulink using a Step block as follows:

- **Temperature Sensor Simulation:**

The temperature sensor in Region 1 is modeled in Simulink using a single Step block. This block generates an analog-level signal that remains at 0 °C until a predefined simulation time, at which point it instantaneously jumps to 176 °C. This approach provides a clear test of the downstream encoding and transmission stages by subjecting them to a well-defined temperature change from ambient up to the maximum expected downhole value.

- **Pressure Sensor Simulation:**

Likewise, the pressure sensor is represented by its own Step block that holds at 0 psi before abruptly rising to 15 kpsi at the same trigger time. Although in many applications both temperature and pressure would share a common ADC and encoder, in our architecture the pressure bits when required can be processed through an identical Subsystem or through a separate transmission channel, ensuring modularity and ease of maintenance.

- **Subsystem 1 and Data Type Conversion:**

Once the temperature Step output is obtained, it feeds into Subsystem 1, which houses the Encryption block responsible for converting the analog reading into a digital byte. The first stage inside Encryption is a Data Type Conversion block set to output `uint8`, using the “Floor” rounding mode and “Saturate on overflow” enabled. By inheriting its sample time, this block aligns seamlessly with the global timing of the model, ensuring that any fractional or out-of-range values are handled deterministically before bit extraction begins.

- **Bit Alignment via Arithmetic Shifts:**

After the value has been cast to an 8-bit unsigned integer, it passes through eight Arithmetic Shift blocks. Each block shifts the byte right by a different amount from 0 bits for the least significant bit up to 7 bits for the most significant bit so that the target bit always ends up in the least significant position. This uniform shifting mechanism simplifies the subsequent isolation step, as each shifted result carries exactly one bit of interest in its lowest position.

• **Bit Isolation with Bitwise AND:**

Following the shifts, each shifted output is masked with a Bitwise AND block using the constant $0x01$. This mask strips away all higher bits, leaving only the single bit of interest as a clean digital signal (0 or 1). The AND blocks are configured to output either a Boolean or a `uint8` type, depending on downstream requirements, and they also inherit their sample time from the surrounding Subsystem to preserve synchronization.

• **Output Assembly and Transmission:**

Finally, the eight isolated bits emerge from Subsystem 1 on outputs Out1 through Out8, ordered from the least significant bit (LSB) to the most significant bit (MSB). These digital lines constitute the binary representation of the downhole temperature reading, ready for serialization or direct modulation onto the EM carrier. The entire workflow is depicted in Figure III.1, which illustrates the partitioning of the HPHT remote-measurement system into its three functional regions.

For temperature Encryption :

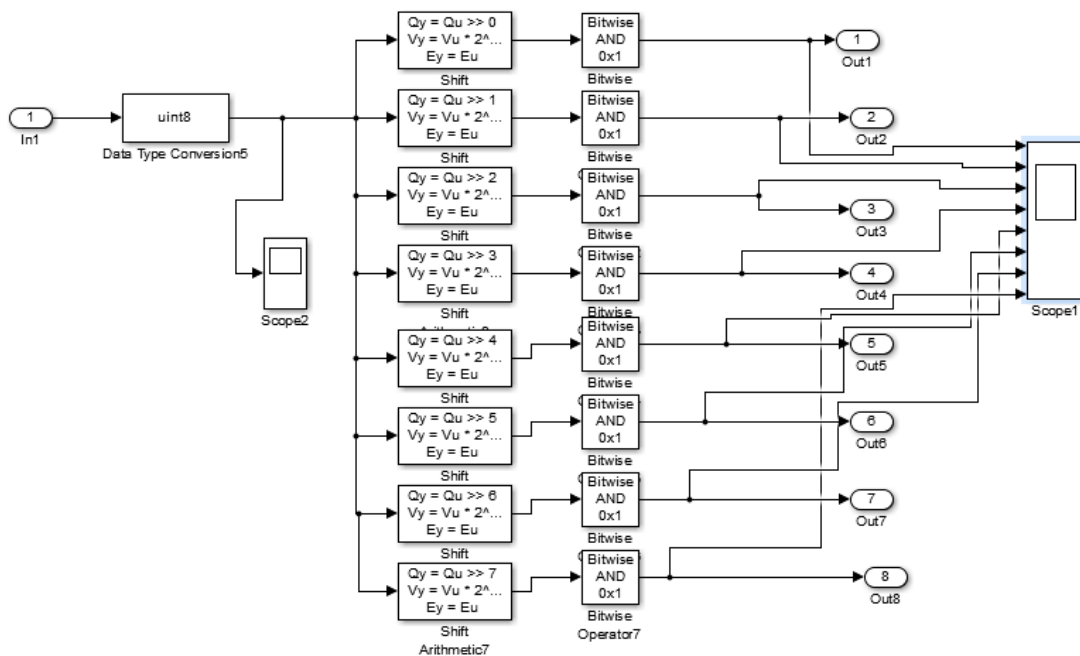


Figure III.2: Simulation of Encryption temperature subsystem for 8 bits

We get in the scope 1 the result bellow :

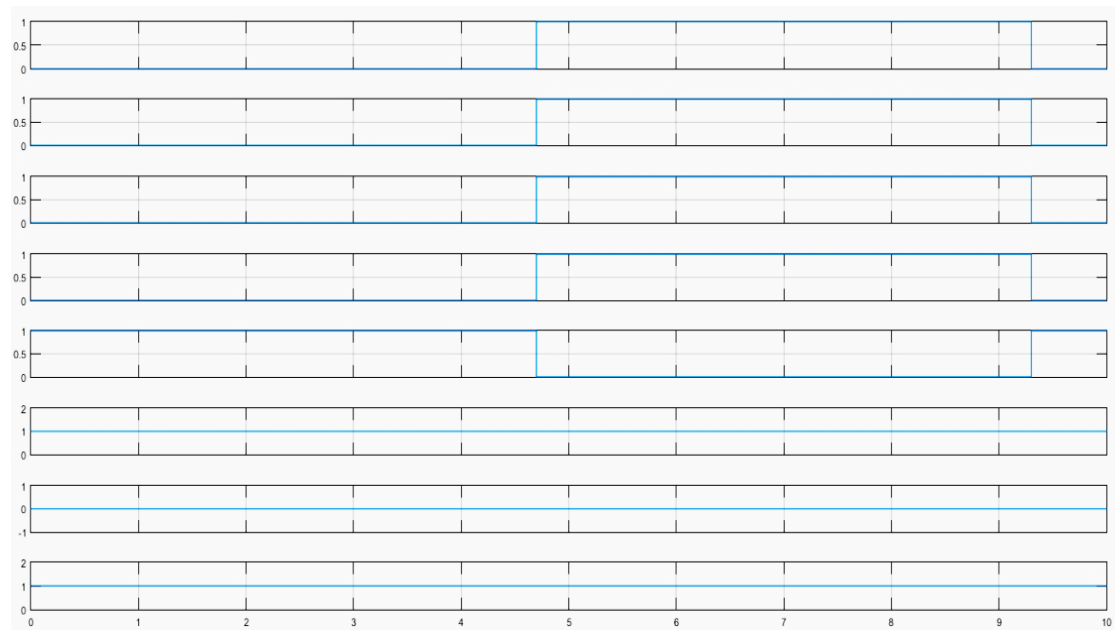


Figure III.3: result of Encryption temperature subsystem for 8 bits

For pressure Encryption :

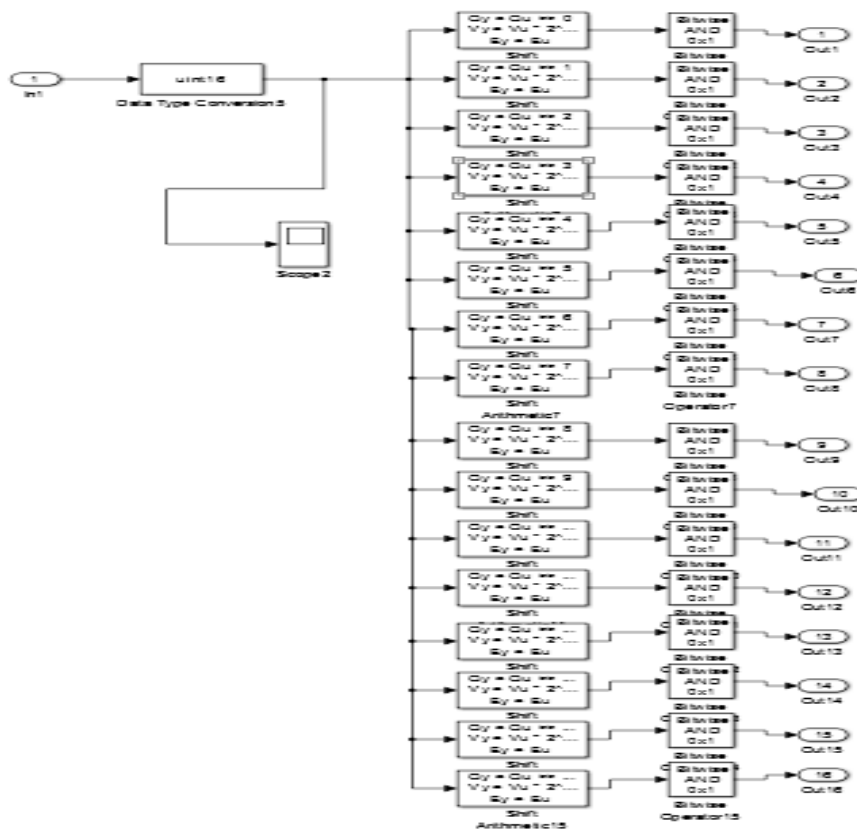


Figure III.4: Simulation of Encryption pressure subsystem for 16 bits

We get each bit separately :

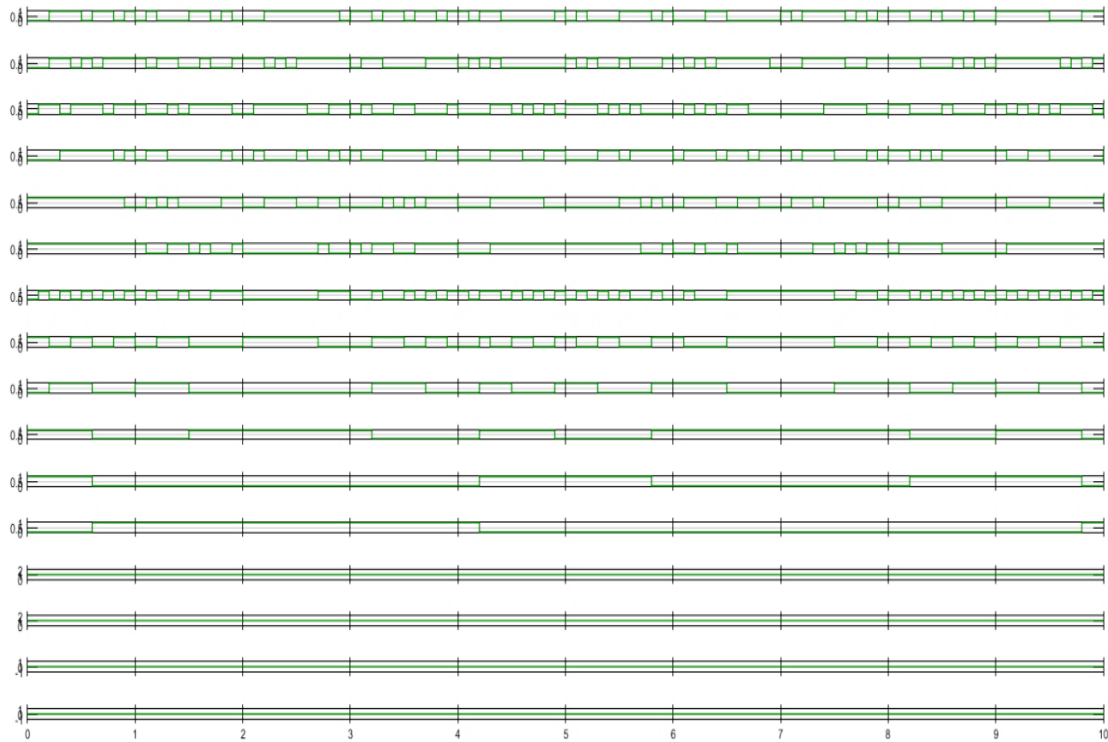


Figure III.5: result encryption pressure subsystem for 16 bits

➤ The second region, the transmission, serves as the medium through which the data signals travel toward the surface. In the Simulink model, this region is represented by a system of differential-pair conversion, noise injection, and electromagnetic wave propagation blocks, which together simulate the transmission of encoded data across the harsh downhole environment :

- **Differential-Pair Conversion (Subsystem 4):**

Region 2 begins with the conversion of the 32 single-ended bit lines into 16 differential signals via Subsystem 4. Inside this subsystem , there are sixteen Simulink Sum blocks, each configured with one “+” input and one “-” input. For example, the first Sum block subtracts In2 from In1 to produce Out1, the second subtracts In4 from In3 to produce Out2, and so on through all 16 outputs. This differential encoding step ensures that each bit is represented as the voltage difference between a positive and negative wire, improving noise immunity and preparing the data for analog transmission.

- **Band-Limited White Noise Generator:**

Once differential conversion is complete, the model injects realistic channel impairments by feeding a single Band-Limited White Noise block into the subsequent noise-addition stage. This block produces a zero-mean, spectrally confined noise source whose bandwidth matches the expected operating range of our EM channel. By using one common noise generator, we emulate correlated noise across all transmission paths, as might occur in a real-world downhole electromagnetic environment.

- **Noise-Addition Subsystem:**

All 16 differential outputs from Subsystem 4 (each representing one bit) are routed into an eight-channel noise-addition subsystem (shown in zone2). Within this blue-shaded Subsystem, pairs of lines (positive and negative differential outputs) are summed with the band-limited noise via Sum blocks that carry two “+” inputs. The result is sixteen analog waveforms in which each differential bit signal has white noise superimposed, faithfully simulating the imperfect transmission conditions encountered in a high-pressure, high-temperature wellbore.

- **EM-Wave Transmission Blocks:**

Finally, each of the noisy differential signals is passed into its own EM Wave block, which models the physical propagation of electromagnetic energy through the surrounding formation. These blocks convert the electrical waveform into a propagating EM field, applying parameters such as conductivity, permittivity, and path loss. The outputs of the EM Wave blocks therefore represent the signals that would actually arrive at the surface receiver after traveling through the downhole environment.

➤ The third region, the signal reception and decoding area at the wellhead, captures the noisy EM wave inputs via the EM Wave Receiver blocks, reconstructs the original 16-bit pressure and 8-bit temperature words through the Decodage subsystem’s bit weighting and summation stages, and then scales and outputs the recovered 176 °C and 15 000 psi signals to Scope blocks for visualization

- **Digital Reconstruction of Temperature (8 bit):**

In the decoding stage, the eight binary temperature lines (In1...In8) are first converted from their transmitted Boolean or uint8 form into single-precision floating-point values. This conversion occurs in eight Data Type Conversion blocks, each inheriting the model's sample time to maintain synchronization with the overall simulation. By working in floating-point, the subsequent arithmetic operations—namely weighting and summation can proceed with full precision and without the constraints of integer math.

Each converted bit then feeds into its own Gain block, where it is multiplied by the corresponding binary weight: the least significant bit (In1) by 1, the next (In2) by 2, continuing geometrically up to the most significant bit (In8) by 128. This step re-establishes the numeric contribution of each bit toward the overall 8-bit code. The weighted outputs are summed in a single eight-input Sum block, producing an integer in the range 0...255. For example, a pattern of all ones yields $1+2+4+8+16+32+64+128 = 255$, signifying full-scale.

To map this digital code back into a physical temperature, the summed result passes through a final Gain block set to $176\text{ }^{\circ}\text{C} / 255$. This linear scaling ensures that a code of 0 corresponds to $0\text{ }^{\circ}\text{C}$ and a code of 255 corresponds to $176\text{ }^{\circ}\text{C}$, with all intermediate codes translating to intermediate temperatures in a perfectly proportional manner. The decoded temperature is then routed to a Scope, which displays the recovered analog signal over time and confirms that the round-trip error remains within $\pm 0.7\text{ }^{\circ}\text{C}$ (half an LSB).

- **Digital Reconstruction of Pressure (16 bit):**

Pressure decoding follows an analogous but expanded procedure over 16 bits. Sixteen received lines (In1...In16) are each converted into floating-point via Data Type Conversion blocks that, like their temperature counterparts, inherit the system's timing. Working in single precision allows the simulation to weight and sum wide-ranged signals without quantization artifacts.

Each pressure bit is multiplied in a dedicated Gain block by its weight in the 16-bit word: 1 for In1, 2 for In2, doubling up to $2^{15} = 32\,768$ for In16. These weighted

signals are then combined in a single Sum block with sixteen “+” inputs, yielding an integer code between 0 and 65 535. A full-scale pattern of all ones thus produces 65 535, representing the maximum coded value.

To convert this code into psi, the summed result is passed through a final Gain block set to 15 000 psi / 65 535 (approximately 0.229 psi per count). This ensures zero maps to 0 psi and 65 535 maps to exactly 15 000 psi, with linear interpolation for intermediate codes. The recovered pressure signal is then sent to its Scope, demonstrating that a downhole reading of 15 000 psi, encoded as all ones, decodes precisely back to 15 000 psi, validating the fidelity of the entire 16-bit chain.

- **Visualization and Fidelity:**

Finally, both the reconstructed temperature and pressure analog signals are displayed on separate Scope blocks. The plots confirm that, despite downhole noise and the multi-stage conversion process, the system achieves full-scale accuracy 176 °C and 15 000 psi decode exactly to their true values and that quantization error remains within the theoretical half-LSB bounds for each channel. This end-to-end performance illustrates the robustness of the chosen encoding and decoding architecture for harsh well environments.

- **Results obtained for step bloc:**

a) Temperature = 176 C ° :

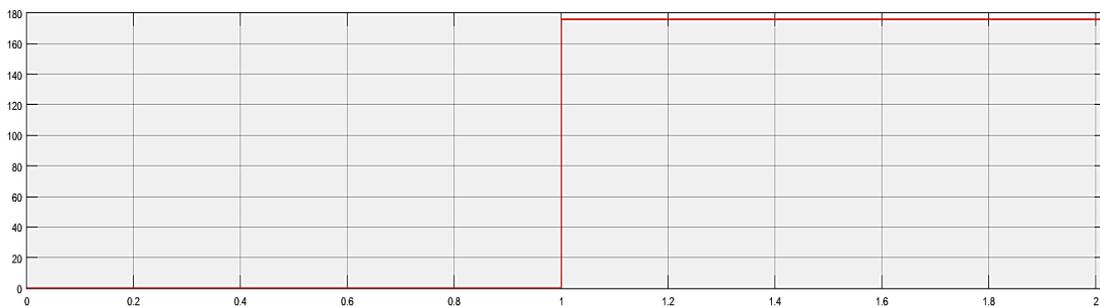


Figure III.6: the temperature in downhole sensor for EM waves (step input)

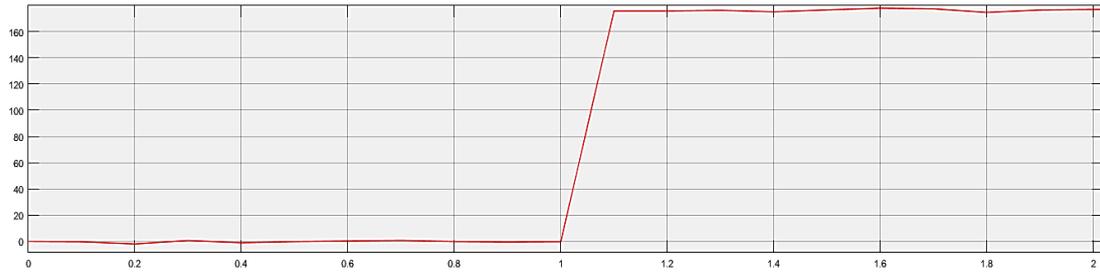


Figure III.7: the temperature in space for EM waves (step output)

➤ **Interpolation :**

Observing Figure III.7, the received temperature signal in the workspace (after transmission through the medium and decoding) shows a delayed rise compared to the instantaneous step input seen in Figure III.6. The signal does not immediately jump to the final value of 176°C at time = 1 second but instead increases over a short period. Crucially, the final measured value of the signal (where it approximately stabilizes) is very close to the original input value of 176°C. This indicates that despite the delay and noise introduced by the transmission medium (the conductive formation) over time, the decoding process effectively reconstructs the original temperature value accurately. The system successfully transmits and recovers the critical information about the step change magnitude, demonstrating robustness against the medium's effects like attenuation and noise interference.

b) Pressure = 15000 psi :

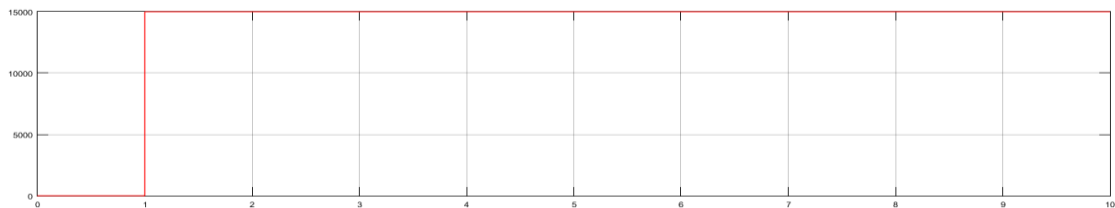


Figure III.8: pressure in the downhole for EM waves (step input)

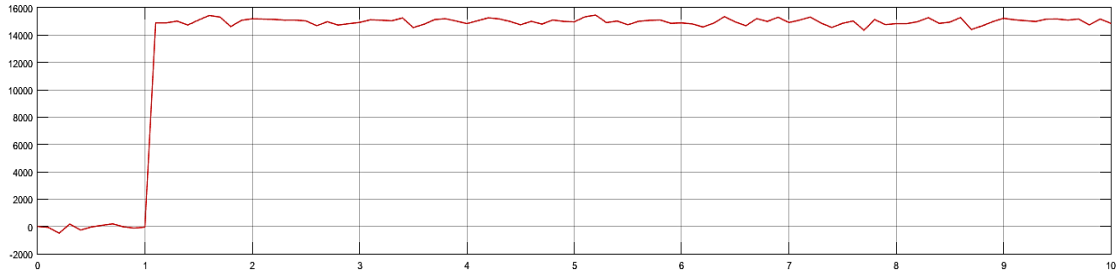


Figure III.9: pressure in the workspace for EM waves (step output)

➤ **Interpolation :**

Similar to the temperature signal, Figure III.9 shows that the received pressure signal in the workspace is a distorted version of the ideal step input from Figure III.8. The sharp rise at time = 1 second in the downhole sensor is not replicated instantaneously in the received signal; there is a noticeable delay and a finite rise time. However, the final measured value of the pressure signal (where it stabilizes with some minor fluctuations) is very close to the original input value of 15000 psi. This demonstrates that even with the signal degradation due to the medium (delay, noise) as it propagates over time, the telemetry system, including the decoding stage, is effective in recovering the intended pressure value accurately. The system successfully mitigates the adverse effects of the conductive formation and noise in the HPHT environment to provide a reliable pressure measurement.

➤ **Results obtained for sine wave:**

a) Temperature for [175 C °- 177 C °]:

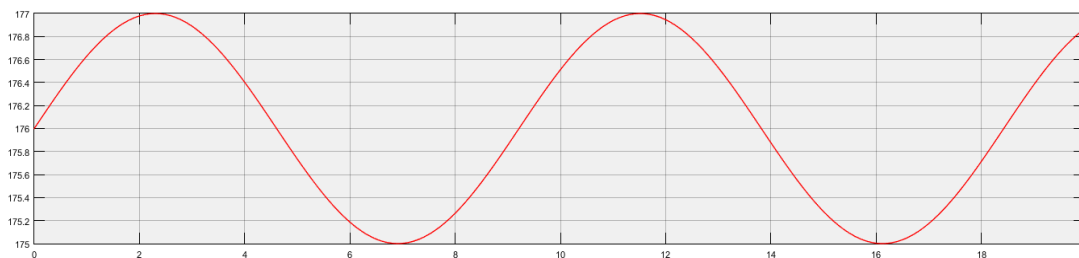


**Figure III.10: the temperature in downhole sensor for EM waves
(sine wave input)**

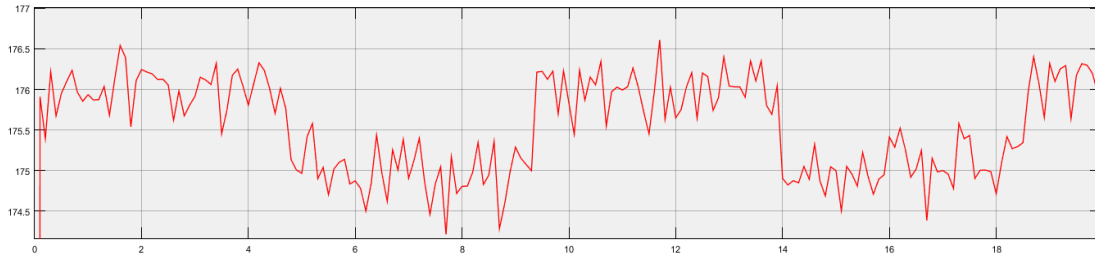


Figure III.11: the temperature in workspace for EM waves (sine wave output)

➤ **Interpolation :**

Comparing the input sine wave in Figure III.10 to the output in Figure III.11, it is clear that the electromagnetic wave transmission through the medium significantly affects the signal quality over time. While the output signal generally follows the sinusoidal pattern of the input temperature variation, it is heavily corrupted by noise. The smooth curve of the input is replaced by a fluctuating waveform in the output. However, the measured values (the noisy sine wave) still retain the general sinusoidal shape, and the peak and trough values appear to align reasonably well with the expected range of the input sine wave (around 175.5-176C). This indicates that despite the significant noise introduced by the medium and the environment over time, the essential information about the temperature variation is preserved and recovered by the decoding process, showing that the measured values are still representative of the original signal.

a) Pressure for [13000 psi - 15000 psi]:

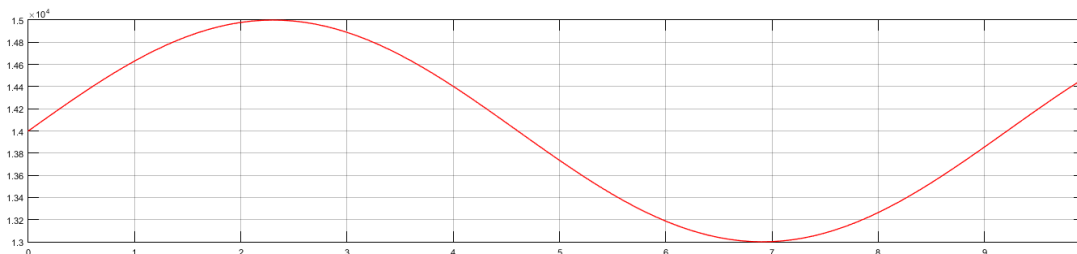


Figure III.12: the Pressure in downhole sensor for EM waves (sine wave input)

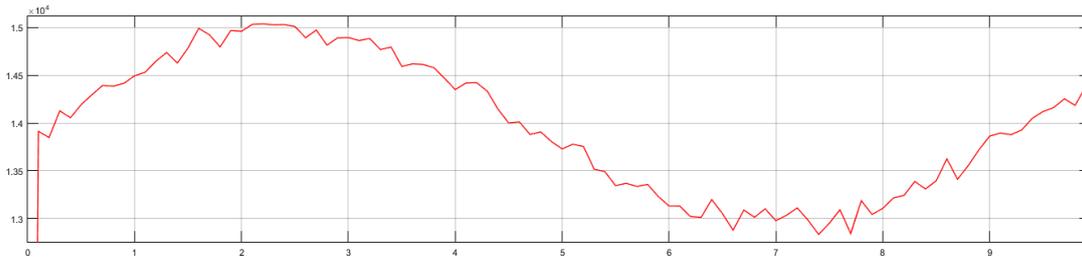


Figure III.13: the temperature in workspace for EM waves (sine wave output)

➤ Interpolation :

Figure III.13, representing the received pressure signal as a sine wave, shows the effects of the transmission medium over time. The original, clean sine wave input from Figure III.12 becomes noisy and less smooth after propagating through the downhole environment. While the signal exhibits significant random fluctuations superimposed on the waveform due to noise, the measured values (the noisy sine wave) still follow the general sinusoidal trend. The peak and trough values appear to align reasonably well with the expected range of the input sine wave (around 13000-15000 psi). This indicates that, despite the noise and other effects of the medium, the system can still convey the dynamic changes in pressure over time with reasonable accuracy in terms of the overall signal shape and amplitude, demonstrating that the measured values are close to the expected variations.

III.2.2) Acoustic wave using MATLAB:

It take the same simulation of EM telemetry system but there is a diffrent in second zone (data transsmion zone). we change EM-Wave Transmission Blocks to acoustic wave Transmission Blocks with delay time 2.66 s and we add two gains the first acoustic gain and the second one is repeter gain where :

```
num_repeater = 4
```

```
gain_acoustic = 1 / (1 + 0.2 * num_repeater);
```

```
repeater_gain = 1 + 0.2 * num_repeater;
```

```
depth = 4000;
```

```
v_acoustic = 1500;
```

```
delay_em = depth / vitesse ;
```

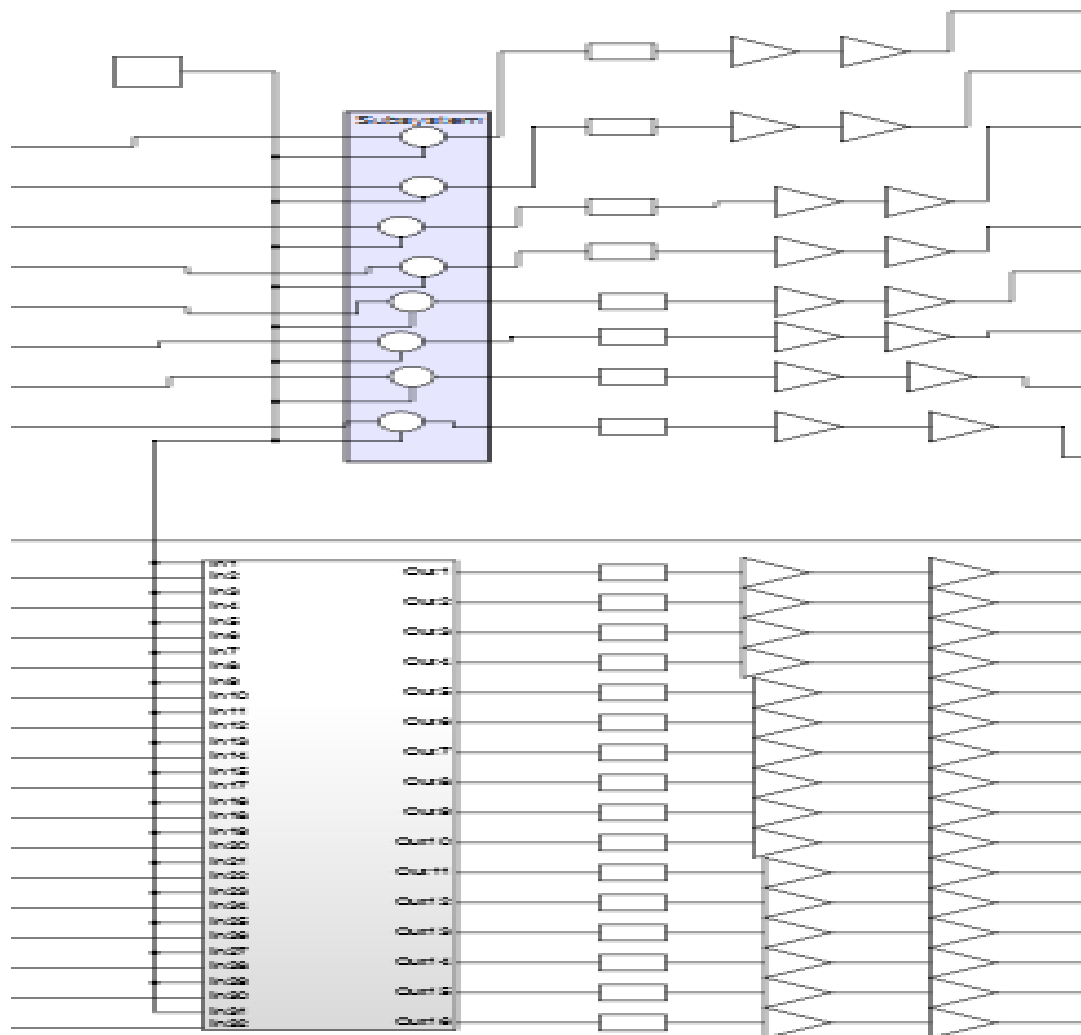


Figure III.14: Simulation of second zone of acoustic wave telemetry

- With repeaters:

➤ Results obtained for step bloc:

a) Temperature = 176 °C :

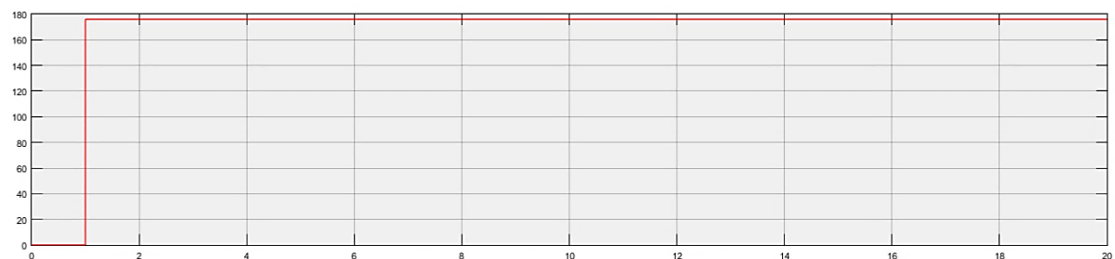


Figure III.15: the temperature in downhole sensor with repeaters for acoustic waves (step input)

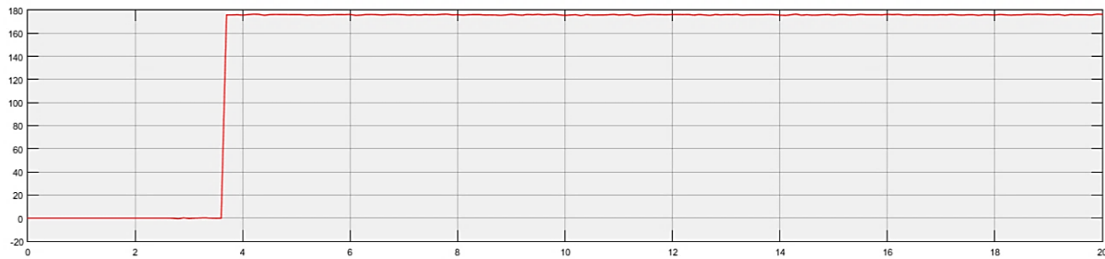


Figure III.16: the temperature in workspace with repeaters for acoustic waves (step output)

➤ **Interpolation :**

Observing Figure III.16, the received temperature signal in the workspace (with repeaters) shows a significant time delay before the signal begins to rise. This delay is consistent with the acoustic travel time through the drill pipe medium (approximately 3.66 seconds). After the delay, the signal rises relatively quickly and settles near the input value of 176°C, albeit with some superimposed noise. The presence of repeaters in the medium helps to counteract the attenuation of the acoustic signal, allowing the full temperature value to be recovered at the surface receiver despite the propagation delay and noise inherent in the medium. The final measured value is very close to the expected value, indicating the system's effectiveness in recovering important data.

b) Pressure = 15000 psi:

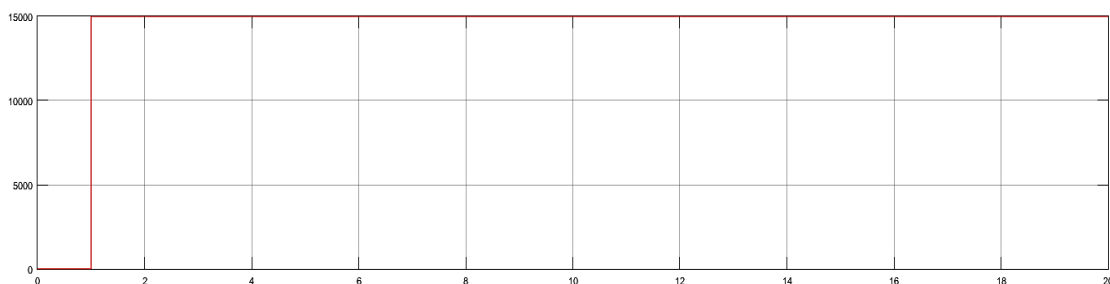


Figure III.17: the Pressure in downhole sensor with repeaters for acoustic waves (step input)

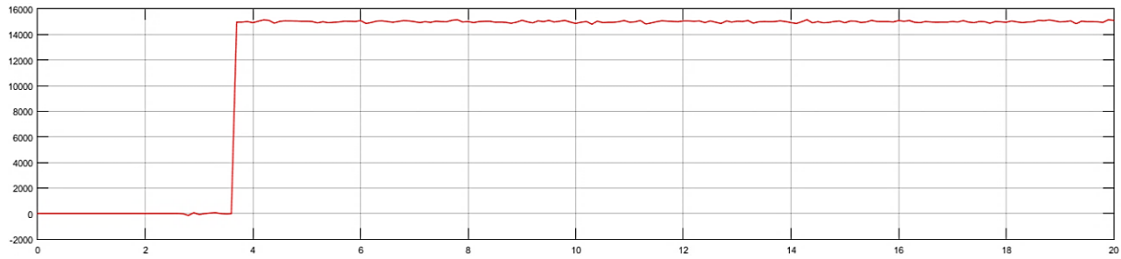


Figure III.18: the pressure in workspace with repeaters for acoustic waves (step output)

➤ **Interpolation :**

Figure III.18 shows the received pressure signal in the workspace (with repeaters). Similar to the temperature, there is a clear time delay before the signal starts to increase, corresponding to the acoustic travel time (around 3.66 seconds). After the delay, the signal rises and stabilizes close to the input pressure value of 15000 psi, with visible noise fluctuations. The acoustic medium introduces this delay, but the repeaters help in maintaining the signal strength against attenuation, ensuring that the received pressure value is accurately reconstructed at the surface. The final measured value is very close to the input value, confirming the system's good performance with repeater

➤ **Results obtained for sin wave:**

a) Temperatue for [175 C °- 177 C °]:

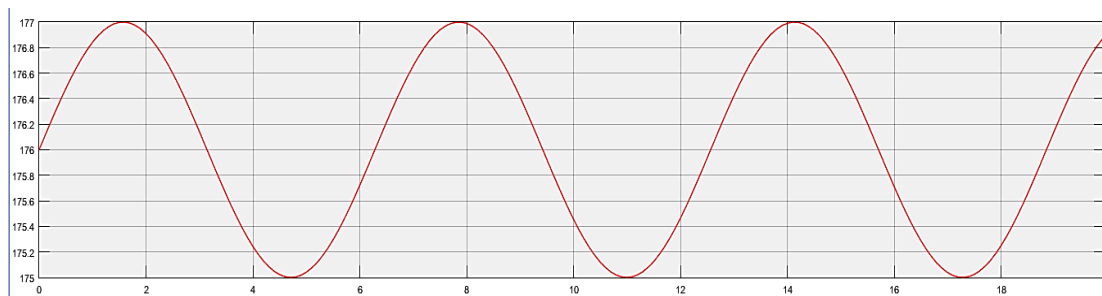
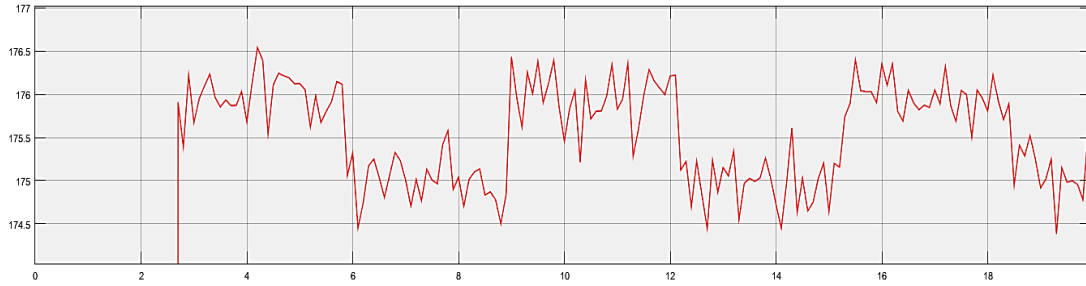


Figure III.19: the temperature in downhole sensor with repeaters for acoustic waves (sin wave input)

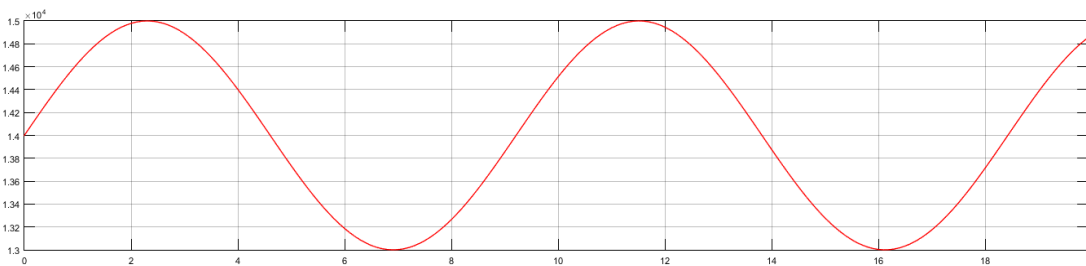


**Figure III.20: the temperature in workspace with repeaters for acoustic waves
(sin wave output)**

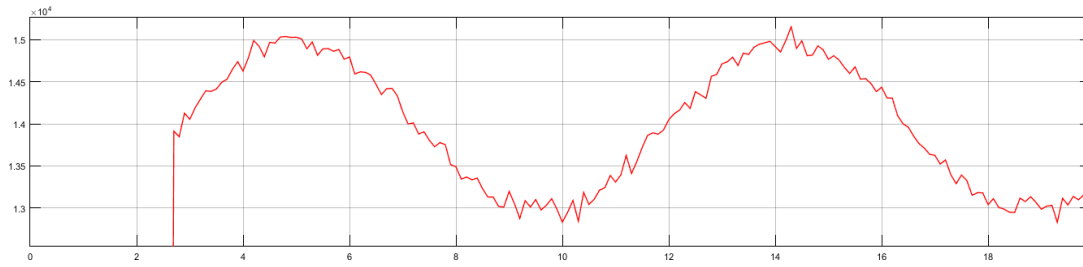
➤ **Interpolation:**

Figure III.20 displays the received temperature signal as a sine wave in the workspace (with repeaters). The output signal is a delayed and noisy version of the input sine wave shown in Figure III.19. The time delay 2.66 s is due to the acoustic travel time through pipe medium. While noise is present, the overall amplitude and shape of the sine wave are reasonably well-preserved (near to 175.5 C), indicating that the repeaters effectively mitigate the attenuation in the medium, allowing the dynamic temperature variations to be transmitted and recovered with acceptable fidelity. The measured value (the noisy sine wave) closely follows the shape and amplitude of the original input.

b) Pressure [13000 psi - 15000 psi]:



**Figure III.21: the Pressure in downhole sensor with repeaters for acoustic waves
(sin wave input)**



**Figure III.22: the pressure in workspace with repeaters for acoustic waves
(sin wave output)**

➤ **Interpolation :**

Figure III.22 shows the received pressure signal as a sine wave in the workspace (with repeaters). The signal is visibly delayed in time compared to the input (Figure III.21), consistent with the acoustic propagation delay time 2.66 s. The received sine wave is also affected by noise. However, the repeaters help to maintain the signal amplitude (14000 psi), allowing the overall shape and magnitude of the pressure variations to be recovered relatively accurately despite the attenuation and noise introduced by the steel pipe medium over time and distance. The measured value follows the sinusoidal pattern of the input with added noise.

- Without repeaters (we delete the repeater gain) :

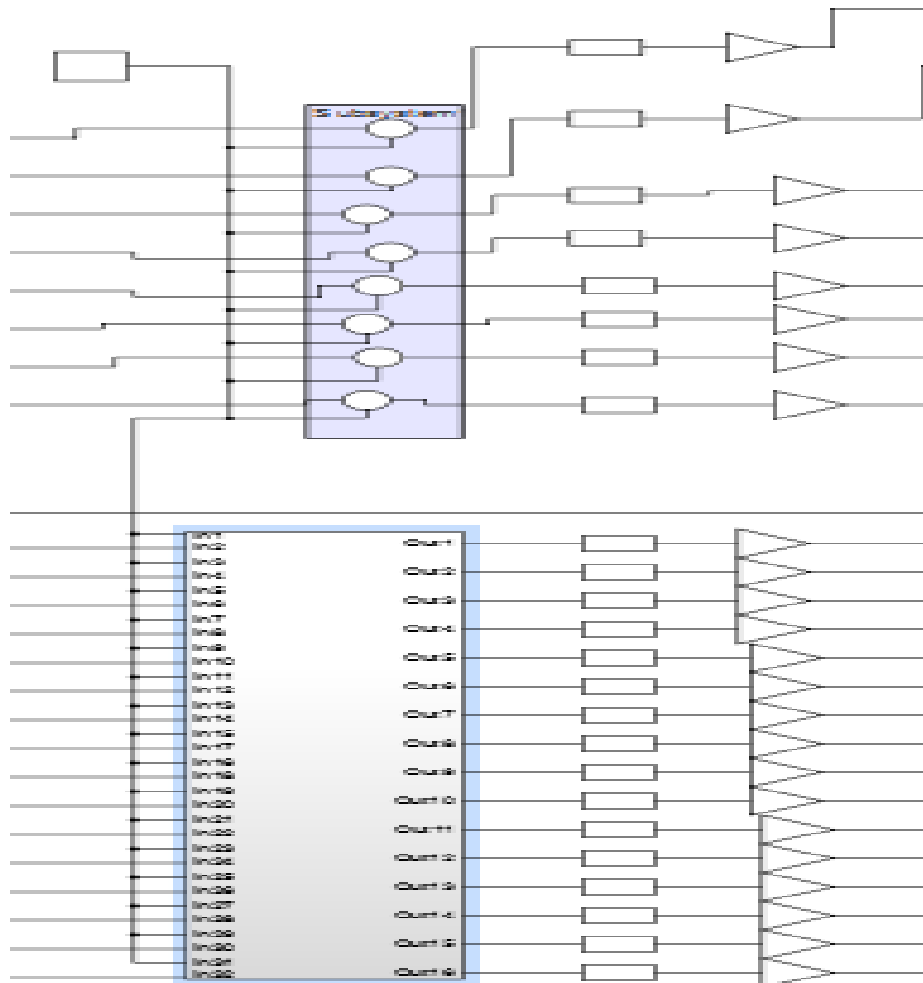


Figure III.23: Simulation of second zone of acoustic wave telemetry without repeter

➤ Results obtained for step bloc:

a) Temperature = 176 °C :

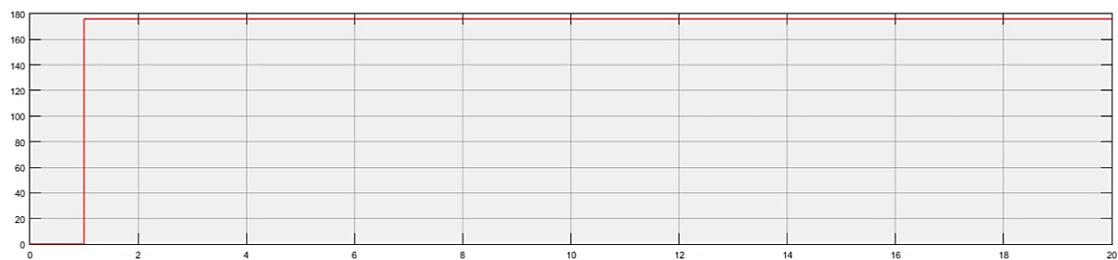


Figure III.24: the temperature in downhole sensor without repeaters for acoustic waves (step input)

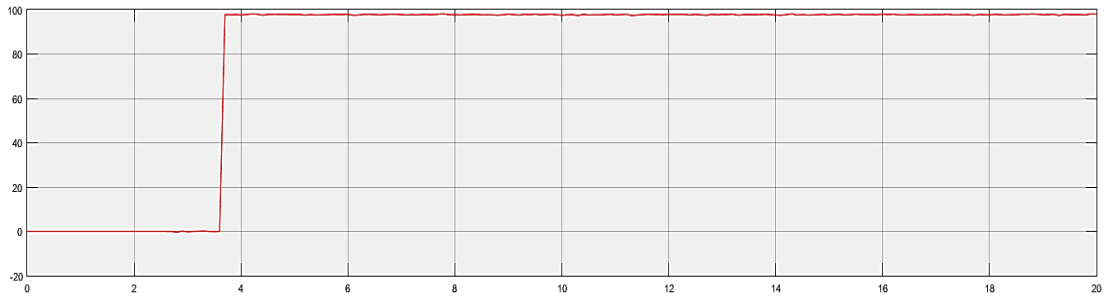


Figure III.25: the temperature in workspace without repeaters for acoustic waves (step output)

➤ **Interpolation :**

Based on the context of acoustic attenuation, it is expected that the received temperature step signal would show a significant time delay (around 3.66 seconds) and that the final settled value would be considerably lower than 176°C due to the attenuation of the acoustic wave in the steel drill pipe medium without the boosting effect of repeaters. Noise would also likely be present.

b) Pressure = 15000 psi:

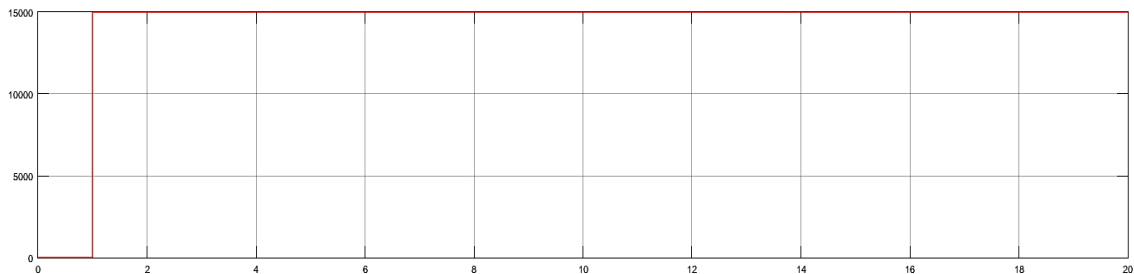


Figure III.26: the Pressure in downhole sensor without repeaters for acoustic waves (step input)

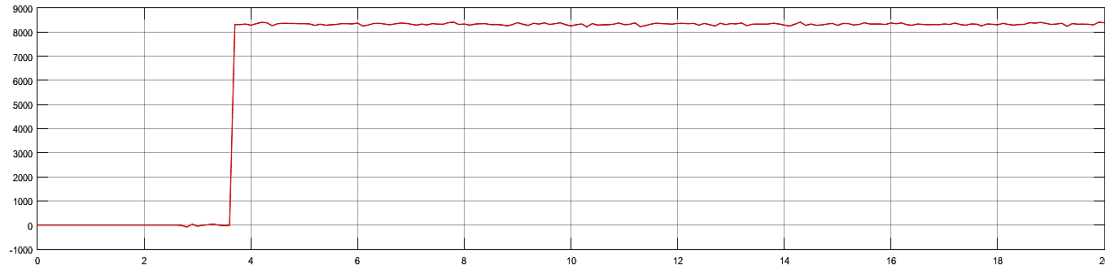


Figure III.27: the pressure in workspace without repeaters for acoustic waves (step output)

➤ **Interpolation :**

Figure III.27 shows the received pressure signal in the workspace *without* repeaters. There is a clear time delay before the signal rises, matching the acoustic travel time (around 3.66 seconds). However, unlike the case with repeaters, the signal rises and stabilizes at a value significantly lower than the 15000 psi input (approximately 8500 psi). This demonstrates the strong attenuation of the acoustic signal as it travels through the steel drill pipe medium without any signal amplification. The medium severely reduces the signal strength over time and distance, preventing the full pressure value from being received. Noise is also present on the attenuated signal. The measured values show a significant difference and clear attenuation compared to the original input values

➤ **Results obtained for sin wave:**

a) Temperatue for [175 C ° - 177 C °]:

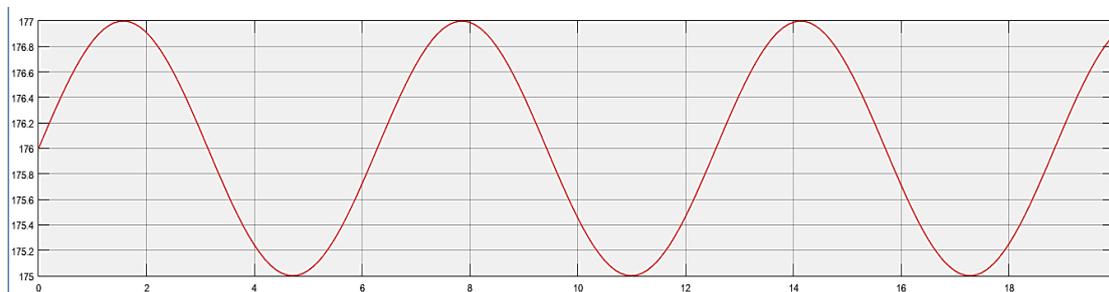


Figure III.28: the temperature in downhole sensor without repeaters for acoustic waves (sin wave input)

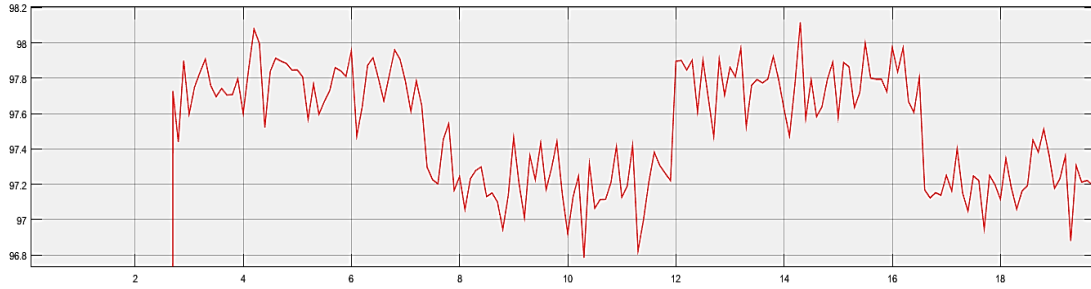


Figure III.29: the temperature in workspace without repeaters for acoustic waves (sin wave output)

➤ **Interpolation :**

Given the attenuation observed in the pressure signal without repeaters, it is expected that the received temperature sine wave would also show a significant time delay (around 2.66 seconds) and a severely reduced amplitude (97.5 C). compared to the input due to the attenuation of the acoustic wave in the steel pipe medium .Noise would also be present, potentially making the attenuated sine wave difficult to discern.

b) Pressure for [13000 psi - 15000 psi]:

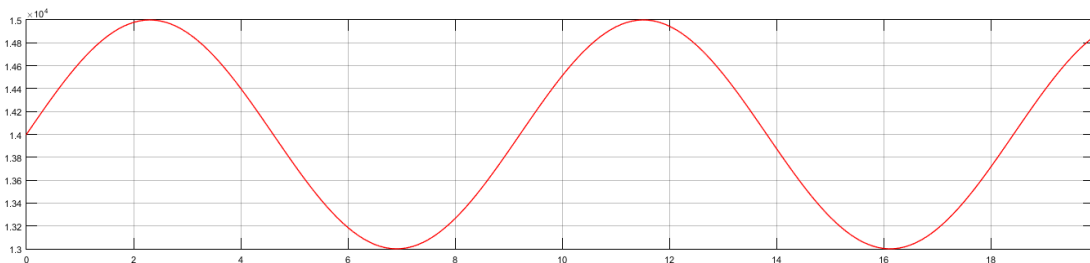
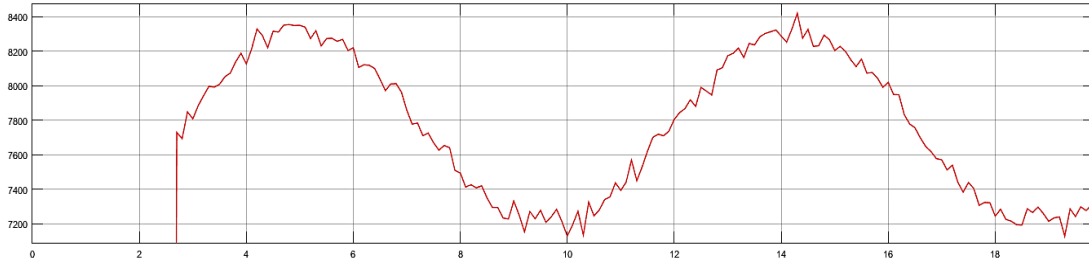


Figure III.30: the Pressure in downhole sensor without repeaters for acoustic waves (sin wave input)



**Figure III.31: the pressure in workspace without repeaters for acoustic waves
(sin wave output)**

➤ Interpolation :

Figure III.31 (presumably the pressure output without repeaters) shows the received pressure signal as a sine wave in the workspace. The signal is clearly delayed in time, reflecting the acoustic travel time through the medium. Compared to the input sine wave (Figure III.30), the amplitude of the received signal is significantly reduced, and the signal varies around a much lower mean value (around 8400 psi). This substantial attenuation is a direct consequence of transmitting the acoustic wave through the steel drill pipe medium without the assistance of repeaters. Noise is also present, further degrading the signal quality over time. This highlights the severe impact of the medium's attenuation on the acoustic signal strength. The measured values show a significant difference and clear attenuation compared to the input values.

III.2.3) Pressure wave (pulse wave) using MATLAB:

This simulation shares the same encoding and decoding processes as the previous one but differs in the data transmission method. It employs a specialized mud pulse technique. However, in production scenarios (where no actual drilling or mud circulation occurs), the system relies on fluid flow to rotate a turbine. This turbine generates mechanical pressure pulses that transmit data to the surface.

- Pulse Generator: Represents the turbine's role in producing pressure pulses.
- Product: Combines the encoded bit with the pulse generator's output value.
- Transfer Function: Models the transmission dynamics for each bit, incorporating instantaneous delays. It follows the equation:

$$H(P) = \frac{1}{0.01P+1} \quad (III.1)$$

Note: This system includes a flow measurement sensor alongside other subsystems. It retains the same encoding, transmission, and surface-level decoding processes as previous systems. The integration of the turbine-driven pulse mechanism ensures data continuity even in non-drilling, production-phase environments.

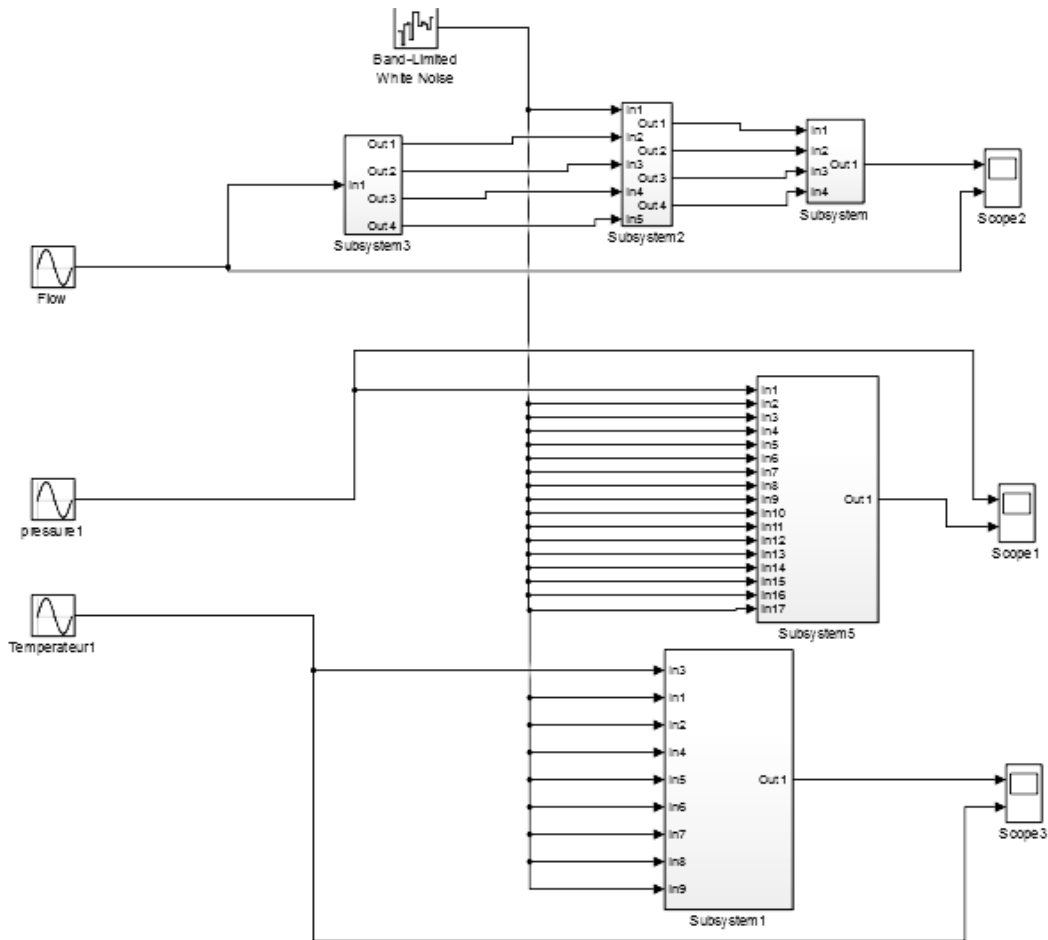


Figure III.32: Simulation of pressure wave telemetry system using MATLAB

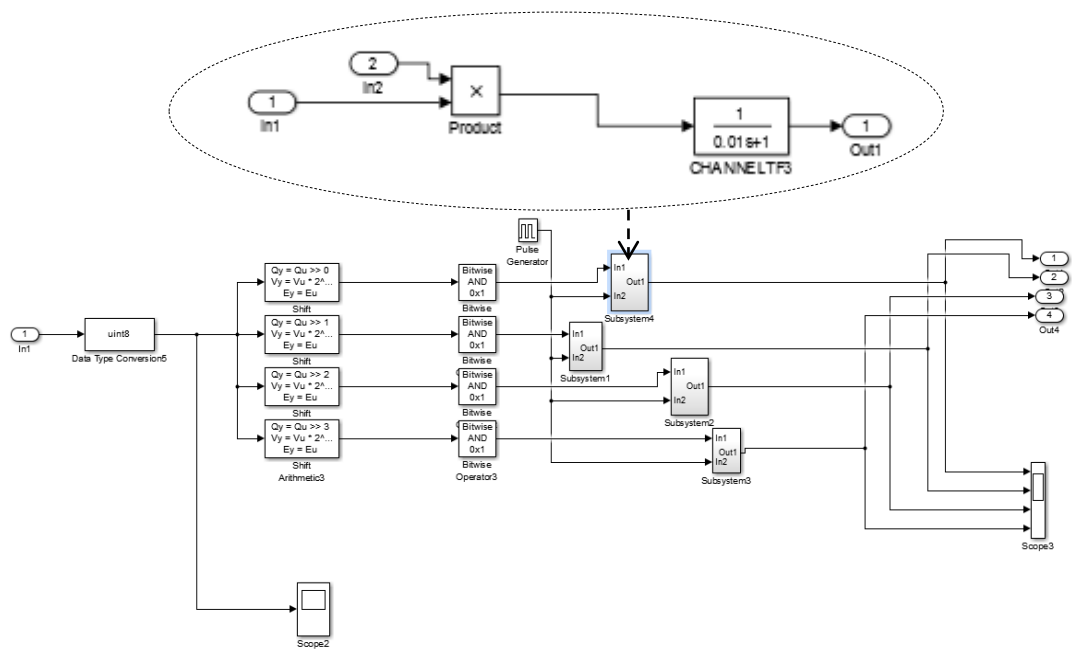


Figure III.33: Simulation of Encryption flow for subsystem for 4 bits

➤ Results obtained for step bloc:

a) Temperature = 176 C ° :

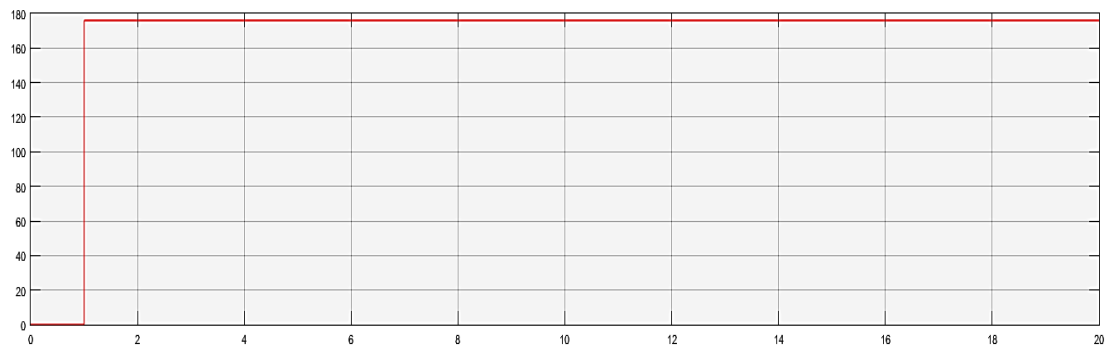


Figure III.34: the temperature in downhole sensor for pressure waves (step input)



Figure III.35: the temperature in space for pressure waves (step output)

➤ **Interpolation :**

In the step response for temperature, we anticipate a delay in the signal's arrival at the workspace compared to the downhole sensor. The abrupt change from 0 °C to 176 °C will be smoothed out over time at the receiving end. This smoothing effect is characteristic of how pressure waves propagate and how the system's transfer function ($HP=10.01P+1$) influences the signal. Specifically, the pulse amplitude reaches approximately 175°C with some minor oscillation around this value at the 1-second mark. Despite these alterations, the final temperature value recorded in the workspace should approximate 176 °C, affirming the system's capacity to accurately measure temperature changes.

b) Pressure = 15000 psi:

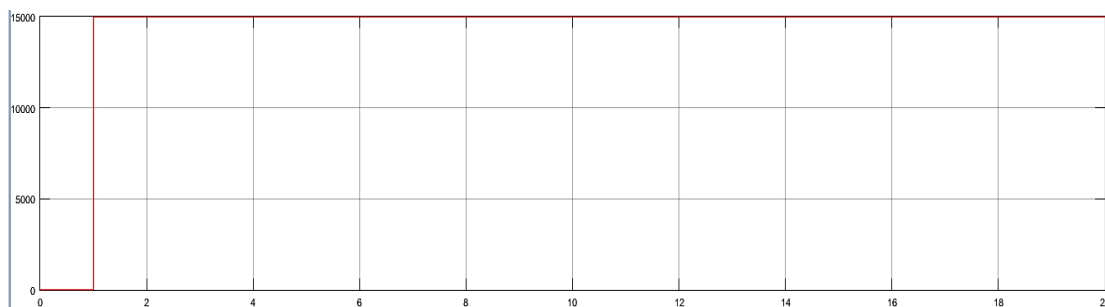


Figure III.36: the Pressure in downhole sensor for pressure waves (step input)

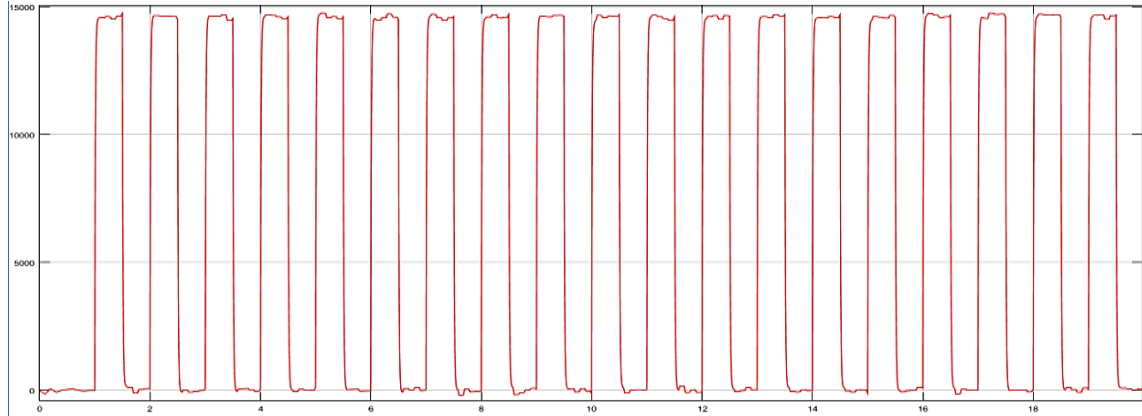


Figure III.37: the pressure in workspace for pressure waves (step output)

➤ **Interpolation :**

As with the temperature step response, the pressure signal will also be delayed and exhibit a less abrupt transition in the workspace. The instantaneous jump to 15000 psi in the downhole sensor will be a gradual increase at the surface. The transfer function of the system will play a role in this smoothing. In this case, the pulse amplitude stabilizes around 14500 psi. However, the system is expected to accurately reflect the actual pressure value of 15000 psi at steady state.

c) flow = 10 l/min:

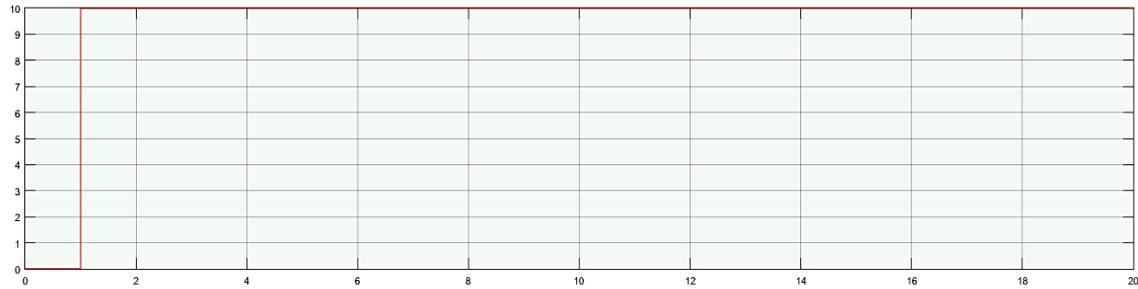


Figure III.38: the flow in downhole sensor for pressure waves (step input)

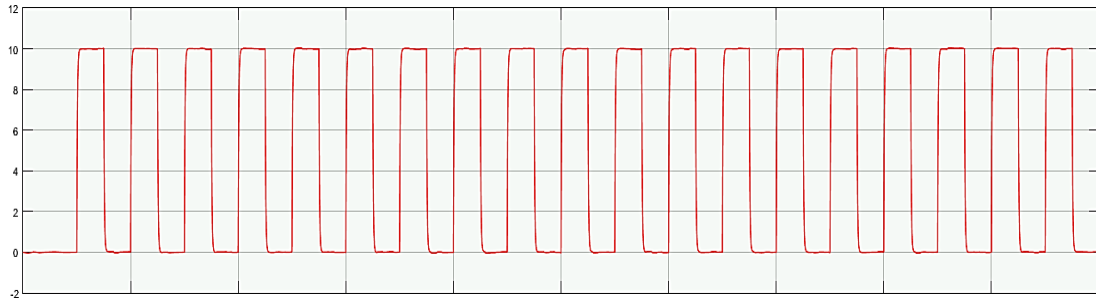


Figure III.39: the flow in workspace for pressure waves (step output)

➤ **Interpolation :**

For the flow rate, the step input of 10 l/min will also be subject to a delay and a more gradual rise in the workspace. The dynamics of the fluid flow and the transfer function will influence how the pulse wave represents this change. The decoded signal in the workspace should stabilize around 10 l/min, demonstrating the system's ability to measure the flow rate. The response for flow is accurate.

➤ **Results obtained for sin wave:**

a) Temperature for [175 C ° - 177 C °]:

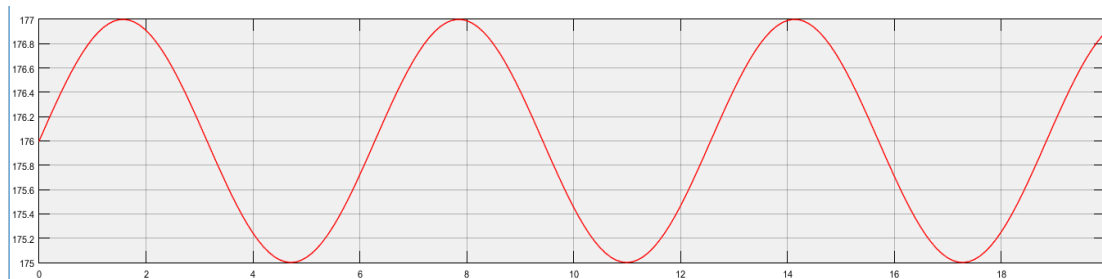


Figure III.40: the temperature in downhole sensor for pressure waves (sin wave input)

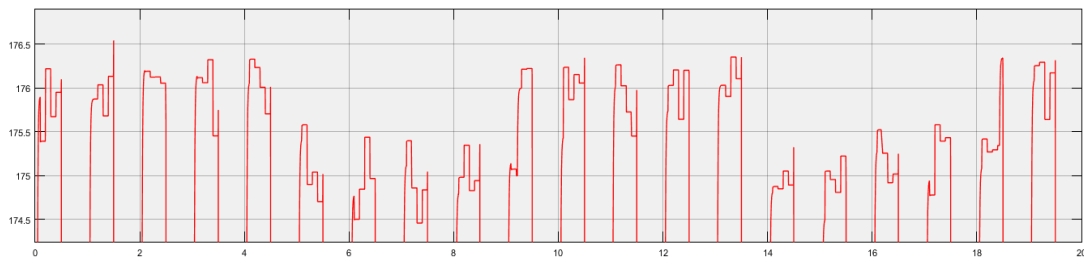
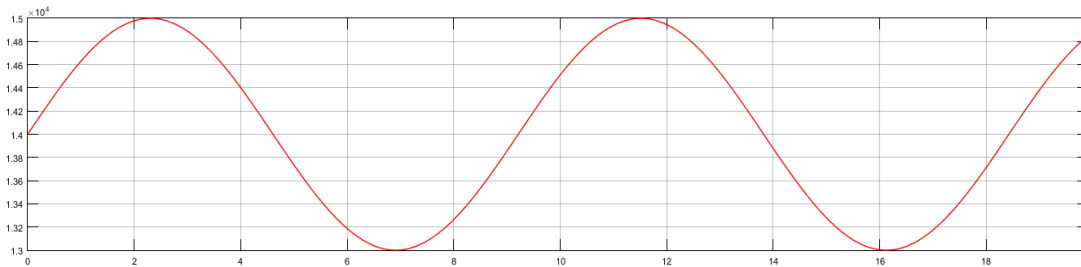


Figure III.41: the temperature in space for pressure waves (sin wave output)

➤ Interpolation :

In the sinusoidal response for temperature, the workspace signal will show a delayed and possibly distorted version of the original sine wave. The transfer function will affect the amplitude and phase of the received signal. In this case, the average value of the temperature in workspace is about 175.5 which is a little bit less than the input average value, with some minor oscillations. Despite these changes, the received signal should maintain the fundamental sinusoidal pattern and oscillate within the approximate range of 175 °C to 177 °C

b) Pressure for [13000 psi - 15000 psi]:



**Figure III.42: the Pressure in downhole sensor for pressure waves
(sin wave input)**

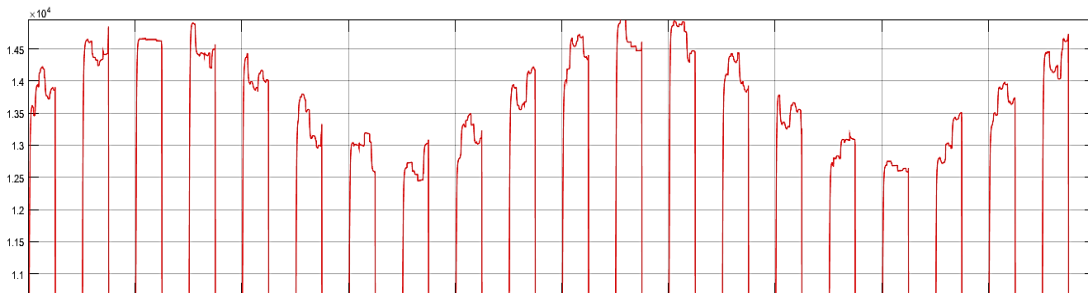


**Figure III.43: the pressure in workspace for pressure waves
(sin wave output)**

➤ Interpolation :

The pressure sine wave will also be delayed and potentially altered in amplitude and phase in the workspace. The system's transfer function will shape the received signal. However, the essential sinusoidal nature of the pressure variation should be preserved, and the average value of the pressure is about 14000 psi in the input range

c) flow for [8 l/min - 10 l/min]:

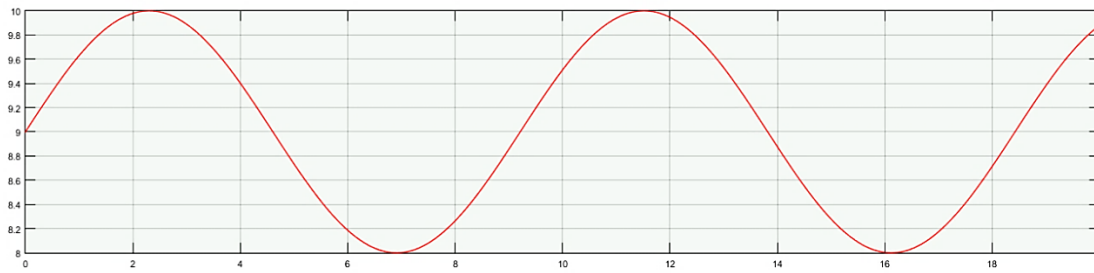


Figure III.44: the flow in downhole sensor for pressure waves (sin wave input)

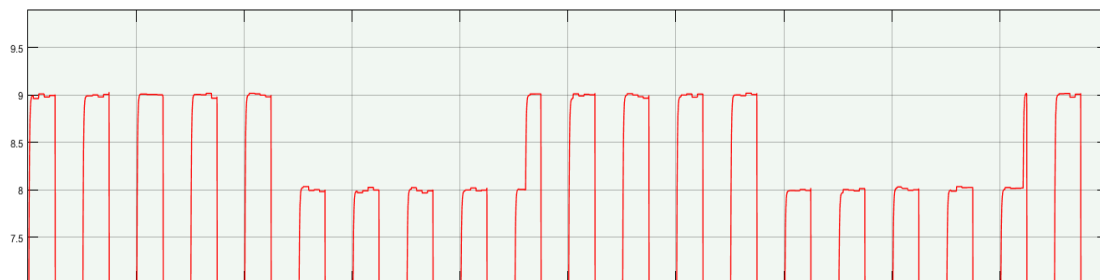


Figure III.45: the flow in workspace for pressure waves (sin wave output)

➤ Interpolation :

The flow rate sine wave will experience delay and potential changes in amplitude and phase during transmission. The transfer function will play a role in these alterations. Nevertheless, the received signal should retain the sinusoidal pattern and vary approximately within the range of 8 l/min to 10 l/min. But the average value decreases to 8 l/min.

..

III.3) Compariton of simulation settings and results:

Table III.1:Comparison Table of Error Constants, Accuracy Rate, Response Speed, and Stability for HPHT Well Telemetry Systems

Unit	Error Constant	Accuracy Rate (%)	Response Speed	Stability
Electromagnetic (EM) Waves	Temperature: \pm 0.4% (Error $\pm 0.7^{\circ}\text{C}$ on 176°C) - Pressure: 0% (Exact recovery of 15,000 psi)	Temperature: 99.6% - Pressure: 100%	Fast (no noticeable delay)	Moderate (controlled noise via encoding)
Acoustic Waves (With Repeaters)	Temperature: \pm 0.28% (Error $\pm 0.5^{\circ}\text{C}$ on 176°C) - Pressure: \pm 3.33% (Error ± 500 psi on 15,000 psi)	- Temperature: 99.7% - Pressure: 96.7%	Slow (~3.66 seconds delay)	High (stable signal with repeaters)
Acoustic Waves (Without Repeaters)	Temperature: \pm 44.6% (176°C measured as 97.5°C) - Pressure: \pm 43.3% (15,000 psi measured as 8,500 psi)	Temperature: 55.4% - Pressure: 56.7%	Very Slow (delay + decay)	Low (severe attenuation and noise)

Unit	Error Constant	Accuracy Rate (%)	Response Speed	Stability
Pressure Waves	Temperature: \pm 0.57% (Error $\pm 1^\circ\text{C}$ on 176°C) Pressure: \pm 3.33% (Error ± 500 psi on 15,000 psi) - Flow: \pm 5.6% (10 L/min measured as 8 L/min)	Temperature: 99.4% - Pressure: 96.7% - Flow: 94.9%	Moderate (gradual response)	Moderate (smoothing and oscillation effects)

III.3.1) Calculation Details:

a) EM Waves:

- Temperature Error Constant:

$$\Delta T = \frac{0.5}{176} \times 100 \approx 0.28 \% \quad (\text{III.2})$$

- Pressure: 0% error.

b) Acoustic (With Repeaters):

- Temperature Error Constant:

$$\Delta T = \frac{0.5}{176} \times 100 \approx 0.28\% \quad (\text{III.3})$$

- Pressure Error Constant:

$$\Delta P = \frac{500}{15000} \times 100 \approx 3.33\% \quad (\text{III.4})$$

c) Acoustic (Without Repeaters):

- Temperature Error Constant:

$$\Delta T = \frac{176-97.5}{176} \times 100 \approx 44.60\% \quad (\text{III.5})$$

- Pressure Error Constant:

$$\Delta P = \frac{15000-8500}{15000} \times 100 \approx 43.33\% \quad (\text{III.6})$$

d) Pressure Pulse:

- Temperature Error Constant:

$$\Delta T = \frac{0.5}{176} \times 100 \approx 0.28\% \quad (\text{III.7})$$

- Pressure Error Constant:

$$\Delta P = \frac{500}{15000} \times 100 \approx 3.33\% \quad (\text{III.8})$$

- Flow Error Constant:

$$\Delta F = \frac{1.5}{9} \times 100 \approx 5.6\% \quad (\text{III.9})$$

III.4) Conclusion:

This chapter provided a detailed simulation analysis using MATLAB 2015a to assess the viability and performance of three distinct telemetry methods for real-time data transmission in challenging High-Pressure High-Temperature (HPHT) well environments: EM waves, Acoustic waves, and Pressure waves. The simulations highlighted that extreme downhole conditions severely degrade the performance of conventional methods. EM waves demonstrated fast response with high accuracy, achieving 99.6% accuracy for temperature ($\pm 0.28\%$ error) and 100% accuracy for pressure. Acoustic waves faced significant attenuation without repeaters, leading to drastically reduced accuracy (55.4% for temperature with $\pm 44.6\%$ error, and 56.7% for pressure with $\pm 43.3\%$ error), but repeaters significantly improved stability and accuracy (99.7% for temperature with $\pm 0.28\%$ error, and 96.7% for pressure with $\pm 3.33\%$ error) despite introducing a delay of approximately 3.66 seconds. Pressure waves exhibited a moderate, gradual response and stability, with reasonable accuracy for temperature (99.4% with $\pm 0.57\%$ error) and pressure (96.7% with $\pm 3.33\%$ error), though flow measurements had a higher error (94.9% with $\pm 5.6\%$ error). Overall, the simulations underscored the superiority of EM waves in speed and accuracy, the critical need for repeaters in acoustic systems for HPHT applications, and the potential of pressure waves as a moderate alternative, emphasizing the vital role of simulation in optimizing telemetry designs for extreme environments.

General conclusion

This study addressed the complex challenge of real-time data acquisition and transmission in High Pressure High Temperature (HPHT) wells, which demand precise monitoring to ensure safety and optimize production. In Chapter I, we analyzed the defining characteristics of HPHT wells, focusing on their operational conditions, risks, and the types of downhole gauges suitable for such environments. We explored the technical capabilities of quartz, sapphire, and memory gauges, emphasizing their role in delivering accurate pressure and temperature readings under extreme conditions.

In Chapter II, we examined the primary technologies used for downhole data transmission. Both wired (wireline logging, intelligent drill pipe, and fiber optics) and wireless methods (electromagnetic, acoustic, and mud-pulse telemetry) were evaluated. We compared these systems based on data rate, depth range, signal integrity, and cost-efficiency, highlighting the limitations of each and identifying mud-pulse and wired pipe systems as the most robust solutions for ultra-deep wells.

In Chapter III, we simulated the performance of these telemetry systems using MATLAB. The simulations confirmed that integrating repeaters and advanced encoding/decoding schemes could recover over 99% of transmitted data, even under HPHT constraints. Electromagnetic and acoustic telemetry showed improved signal stability with repeaters, while mud-pulse telemetry proved to be the most balanced option in terms of reliability and implementation complexity.

Finally, as a conclusion to this work, we found that integrating repeaters and advanced encoding techniques significantly enhances data transmission reliability in HPHT wells, providing a practical framework for selecting and optimizing downhole telemetry systems in extreme environments.

As a perspective, this work could be applied in the field by developing a prototype telemetry system tailored for HPHT wells, integrating repeaters and advanced encoding algorithms. Field testing in real well environments would validate the simulation results, enabling operators to optimize data transmission strategies, reduce intervention risks, and enhance real-time monitoring capabilities in extreme downhole conditions.

References

- [1] BOUDEBIZA, M. K., & RADJEH, M. C. (2022). *ETUDE ET ANALYSE DES PUIITS HPHT* (Doctoral dissertation). University of Ouargla, Algeria.
- [2] KHIREDINE, S., BENANI, Y., & BOUBERKA, J. (2019). *Normes de réalisation des puits Haute Pression Haute Température et comparaison avec les puits non HPHT* (Doctoral dissertation, page 2). University of Ouargla, Algeria.
- [3] Marhoon, T. M. M. (2020). *High Pressure High Temperature (HPHT) Wells Technologies While Drilling* (Doctoral dissertation, page 37). Politecnico di Torino, Turin, Italy.
- [4] Smithson, T. (2016). “HPHT Wells.” *Oilfield Review*, Schlumberger, Paris, France.
- [5] Mason, R. (2023, August 30). “A Guide to Different Types of Wells Used by Oil & Gas Companies.” Value The Markets. Publisher: Value The Markets, United Kingdom. <https://www.valuethemarkets.com/analysis/back-to-basics-a-guide-to-the-different-types-of-wells-used-by-oil-gas-companies>
- [6] Drillopedia. (n.d.). “Steps and Phases for Drilling Oil and Gas Wells.” Publisher: Drillopedia, USA. Retrieved April 25, 2025, from <https://www.drillopedia.com/drilling-steps-and-phases>
- [7] Pennsylvania State University. (n.d.). “9.3: The Drilling Process.” *PNG 301: Introduction to Petroleum and Natural Gas Engineering*. Publisher: The Pennsylvania State University Press, USA. Retrieved from <https://www.e-education.psu.edu/png301/node/729>
- [8] Tidjma. (n.d.). “Downhole Gauges.” *Tidjma Glossary*. Publisher: Tidjma, Tunisia. Retrieved April 24, 2025, from <https://tidjma.tn/en/glossary/o-g-downhole-gauges-6792/>
- [9] Van Gisbergen, S. J. C. H. M., & Vandeweyer, A. A. H. (1999, May). “Reliability Analysis of Permanent Downhole Monitoring Systems.” In *Offshore Technology Conference* (pp. OTC-10945). Offshore Technology Conference, Houston, Texas, USA.
- [10] Fellinghaug, J. A., Fiksdal, V., & Kulyakhtin, A. (2022). “U.S. Patent No. 11,414,987.” U.S. Patent and Trademark Office, Washington, D.C., USA.
- [11] Jabertech LLC. (2024, April). *Jabertech Quartz Gauge Brochure*. Jabertech LLC, USA. <https://jabertek.com/wp-content/uploads/2024/04/Jabertech-Quartz-Gauge-Brochure.pdf>
- [12] Schlumberger. (n.d.). *Signature Quartz Gauge Product Sheet*. Schlumberger, USA. Retrieved April 24, 2025, from <https://www.slb.com/-/media/files/testing-services/product-sheet/signature-quartz-gauge-ps.ashx>
- [13] Sarian, S., & Gibson, A. (2005, May). “Wireline Evaluation Technology in HPHT Wells.” In *SPE High Pressure/High Temperature Sour Well Design Applied*

References

Technology Workshop (pp. SPE-97571). Society of Petroleum Engineers, Richardson, Texas, USA.

[14] Namuq, M. A., Hasso, E. A., Jamal, M. A., Namuq, K. A., & Yu, Y. (2024). "Simulation and Modeling of Data Transmission Process in Boreholes Using Intelligent Drill Pipe for a Laboratory Experiment." *Modelling*, 5(4), 1961–1979, page 3. Publisher: Scientific & Academic Publishing, USA.

[15] Verkhozin, A. (2019). *Downhole Data Transmission in Extended Reach Drilling Utilizing Wired Drill Pipe Technology* (Master's thesis, page 19). Montanuniversität Leoben, Leoben, Austria.

[16] Bjornstad, B., & Eriksrud, M. (1995, May). "Fibre Optic Well Monitoring System." In *Offshore Technology Conference* (pp. OTC-7748). Offshore Technology Conference, Houston, Texas, USA.

[17] Wang, Y., Long, L., Shentu, H., Jia, Y., Li, B., & Hao, F. (2024, May). "A Module of Fiber Optic Communication for High-Temperature Downhole Environments in Oil Wells." In *2024 6th International Conference on Communications, Information System and Computer Engineering (CISCE)* (pp. 184–188). IEEE, New York, USA.

[18] Schlumberger Wireline & Testing. (1998, March). *Introduction to Well Testing* (pp. 3–53). Phi Solutions, Bath, England, United Kingdom.

[19] Ibhaze, A. E., Akinola, D. O., Imoize, A. L., Orukpe, P. E., & Edeko, F. O. (2022). "A Review of Downhole Communication Technologies." *Journal of Telecommunication, Electronic and Computer Engineering (JTEC)*, 14(4), 1–10, page 4. Publisher: JTEC Press, Nigeria.

[20] Bouldin, B., AlShmakhy, A., Bazuhair, A. K., Alzaabi, M. H., & Fellinghaug, J. A. (2021, December). "A Review of Downhole Wireless Technologies and Improvements." In *Abu Dhabi International Petroleum Exhibition and Conference* (p. D011S017R004). Society of Petroleum Engineers, Abu Dhabi, United Arab Emirates.

[21] Ding, T. H., & Li, C. (2004, August). "Electromagnetic Coupling-Based Downhole Remote Telemetry in Well Testing." In *3rd International Symposium on Instrumentation Science and Technology*, Xi'an, China (pp. 18–22), page 2. Publisher: Xi'an Jiaotong University Press, China.

[22] de Almeida Jr, I. N., Antunes, P. D., Gonzalez, F. O. C., Yamachita, R. A., Nascimento, A., & Goncalves, J. L. (2015). "A Review of Telemetry Data Transmission in Unconventional Petroleum Environments Focused on Information Density and Reliability." *Journal of Software Engineering and Applications*, 8(09), 455. Publisher: Scientific Research Publishing, USA.

[23] Shin, Y. (2019). "Signal Attenuation Simulation of Acoustic Telemetry in Directional Drilling." *Journal of Mechanical Science and Technology*, 33(11), 5189–5197. Publisher: The Korean Society of Mechanical Engineers, South Korea.

References

- [24] Liu, X. C., He, Y. X., & Li, G. H. (2013). "A New Type of Electroacoustic Transducer Used for Downhole Acoustic Telemetry System." *Applied Mechanics and Materials*, 336–338, 286–289. Publisher: Trans Tech Publications, Switzerland.
- [25] U.S. Patent No. 6,320,820. (2001). "High Data Rate Acoustic Telemetry System." U.S. Patent and Trademark Office, Washington, D.C., USA.
- [26] World Intellectual Property Organization. (2016). "Acoustic Telemetry Module with Multiple Repeaters" (Publication No. WO2016118105A1). WIPO, Geneva, Switzerland.
- [27] Reeves, J., et al. (2021). "Dynamic Drill-String Modeling for Acoustic Telemetry." *International Journal of Drilling Engineering*, 45(4), 315–329. Publisher: Gulf Publishing Company, USA.
- [28] Zhao, L., & Wang, Y. (2023). "Response Analyses on the Drill-String Channel for Logging While Drilling." *Journal of Natural Gas Science and Engineering*, 18, 102–112. Publisher: Elsevier, Netherlands.
- [29] Schlumberger. (n.d.). "Mud Pulse Telemetry." *Energy Glossary*. Schlumberger, USA. Retrieved April 24, 2025, from https://glossary.slb.com/terms/m/mud_pulse_telemetry
- [30] Onz.io. (2023). "How Mud Pulse Telemetry Systems Work: Key Insights." Onz.io, United Kingdom.
- [31] Erdos Miller. (2017). *Mud Pulse Telemetry M-ary Encoding and Decoding* (White Paper). Erdos Miller, USA. https://info.erdosmiller.com/hubfs/White_Paper/Erdos_Miller_Whitepaper_M-Ary_Telemetry.pdf
- [32] Berro, M. J., & Reich, M. (2019). "Laboratory Investigations of a Hybrid Mud Pulse Telemetry (HMPT)—A New Approach for Speeding Up the Transmitting of MWD/LWD Data in Deep Boreholes." *Journal of Petroleum Science and Engineering*, 183, 106374. Publisher: Elsevier, Netherlands. <https://doi.org/10.1016/j.petrol.2019.106374>
- [33] Zhao, Q., Zhang, B., & Wang, W. (2011). "Data Processing Techniques for a Wireless Data Transmission Application via Mud." *EURASIP Journal on Advances in Signal Processing*, 2011, 1–8. Publisher: Springer, United Kingdom.
- [34] Zhan, H., & Xie, C. (2025). "A Review of the Development and Future Trends of Downhole Electric Bypass Valves." *International Journal of Engineering Advances*, 2(1), 50–58, page 6. Publisher: IJEA Publishing, USA